Titre: Title:	Integration of Viscoplastic Effects in Nonlinear Ground Response Analysis
Auteur: Author:	Mallak Janati Idrissi
Date:	2019
Type:	Mémoire ou thèse / Dissertation or Thesis
Référence: Citation:	Janati Idrissi, M. (2019). Integration of Viscoplastic Effects in Nonlinear Ground Response Analysis [Master's thesis, Polytechnique Montréal]. PolyPublie. https://publications.polymtl.ca/3845/

POLYTECHNIQUE MONTRÉAL

affiliée à l'Université de Montréal

Integration of viscoplastic effects in nonlinear ground response analysis

MALLAK JANATI IDRISSI

Département des génies civil, géologique et des mines

Mémoire présenté en vue de l'obtention du diplôme de *Maîtrise ès sciences appliquées*

Génie civil

Avril 2019

POLYTECHNIQUE MONTRÉAL

affiliée à l'Université de Montréal

Ce mémoire intitulé:

Integration of viscoplastic effects in nonlinear ground response analysis

présenté par **Mallak JANATI IDRISSI**

en vue de l'obtention du diplôme de *Maîtrise ès sciences appliquées*

a été dûment accepté par le jury d'examen constitué de:

Bruno MASSICOTTE, président

Samuel YNIESTA, membre et directeur de recherche

Carlos OVALLE, membre

ACKNOWLEDGEMENTS

I would first like to thank my supervisor Samuel Yniesta for his constant support during my master, for his patience, his immense knowledge and his motivation. His advice helped me throughout the research and writing of this thesis, he directed me in the right direction whenever he thought I needed it and I could not have imagined having a better advisor and mentor for my master study.

The environment of Polytechnique Montreal has allowed me to develop academic, professional and personal skills. That's why I want to thank the great people I met. Elsa Antoine was a tremendous moral support and reassured the doubts that I felt about my research project. With Mohammad Zarrabi, we worked long days at the office where we had inspiring exchanges and for that I am grateful to him.

Finally, I must express my deep gratitude to my parents for their unwavering support and continued encouragement throughout my years of study and through the process of researching and writing this thesis. Despite the distance, they knew how to be present and this accomplishment would not have been possible without them.

RESUME

Les analyses non-linéaires du comportement unidimensionnel des dépôts de sol permettent d'évaluer le potentiel d'amplification des ondes sismiques d'un site, et requièrent des lois de comportement qui contrôlent la réponse du sol aux chargements sismiques. Ces lois de comportement utilisent généralement les courbes de réduction du module de cisaillement et d'amortissement comme paramètres d'entrée, où la courbe de réduction du module de cisaillement représente la diminution de la rigidité du sol en fonction de la déformation, et la courbe d'amortissement représente la capacité du sol à dissiper l'énergie lors de cisaillement cyclique.

Les lois de comportement sont évaluées par leur capacité à reproduire les courbes d'entrée d'amortissement et de réduction du module de cisaillement, mais la plupart des modèles échouent à obtenir une reproduction parfaite de ces courbes. La plupart des modèles utilisent par exemple les règles de Masing modifiées (Masing 1926) pour correspondre à la courbe d'amortissement d'entrée, mais cela ne garantit pas un parfait ajustement de la courbe d'amortissement. Récemment, Yniesta et al. (2017) ont présenté le modèle ARCS, qui est un modèle de contrainte-déformation non-linéaire unidimensionnelle capable de reproduire n'importe quelle courbe d'entrée d'amortissement ou de réduction du module de cisaillement. Cependant, ce modèle, ainsi que les autres modèles utilisés dans les analyses de réponse de dépôts, sont indépendants du taux de déformation. Or, il a été prouvé que le comportement du sol est fortement dépendant du taux de déformation pendant les chargements monotones et cycliques.

Dans ce mémoire, je présente un nouveau modèle viscoplastique capable d'inclure la dépendance du comportement du sol au taux de déformation pour l'analyse unidimensionnel des réponses de dépôts de sol. Les équations constitutives du modèle viscoplastique sont dérivées de manière à ce que la réponse du modèle soit cohérente avec le comportement rapporté dans la littérature concernant les effets visqueux. Le modèle comprend deux parties: une réponse non visqueuse et une réponse visqueuse. La partie non visqueuse est basée sur le modèle ARCS et la partie visqueuse inclue la dépendance au taux de déformation. Des exemples de simulations d'un seul élément du sol sont présentés afin d'étudier les prédictions typiques du modèle.

Le modèle viscoplastique est implémenté dans Deepsoil, un logiciel d'analyse de comportement unidimensionnel des dépôts de sol. Le modèle est validé en simulant dans Deepsoil un test de

centrifugeuse représentant un problème d'analyse de la réponse d'un dépôt de sol. Les résultats sont comparés en termes de réponse spectrale, de spectre de résidus et de fonctions de transfert. Les résultats montrent une nette amélioration des prédictions quand le taux de déformation est pris en compte dans l'analyse non-linéaire de la réponse d'un dépôt de sol, comparé au modèle non visqueux.

ABSTRACT

Nonlinear one-dimensional ground response analyses are used to assess the potential of ground motion amplification at a site, and require constitutive models that control the response of the soil to seismic loading. Constitutive models typically use modulus reduction and damping curves as input parameters where the modulus reduction curve represents the decrease of stiffness of the soil with shear strain, and the damping curve represents the capacity of the soil to dissipate energy uponcyclic shearing.

The models are evaluated by their ability to match their input modulus reduction and damping curves, but most of the existing models tend to introduce a misfit of either of these curves. For instance, most models use modified Masing rules (Masing 1926), to match the input damping curve but are unable to ensure a perfect fit of the damping curve. Recently, Yniesta et al. (2017) introduced the ARCS model, a one-dimensional nonlinear stress-strain model capable of reproducing any user-input modulus reduction and damping curve. However, this model, and the other models used in ground response analyses arestrain-rate independent, but it has been proved that soil behaviour is highly strain-rate dependent during both monotonic and cyclic loading.

This thesis presents a new viscoplastic model capable of capturing strain rate dependence of the soil's behaviour for 1D ground response analysis. The constitutive equations of the viscoplastic model are derived so that the response of the model is consistent with the behaviour reported in the literature regarding viscous effects. The model is divided in two parts: the inviscid and the viscous response. The inviscid part is based on the ARCS model and the viscous part includes the strain-rate dependency. Examples of single element simulations are presented in order to study the typical predictions of the model.

The proposed viscoplastic model is implemented in Deepsoil, a one-dimensional ground response analysis program. The model is validated by simulating in Deepsoil a centrifuge test representing a 1D ground response analysis problem. The results are compared in terms of spectral response, spectral residuals and transfer functions. The results show a clear improvement of the predictions when considering the strain-rate dependency in nonlinear ground response analysis, as compared to the inviscid model.

TABLE OF CONTENTS

LIST OF TABLES

LIST OF FIGURES

LISTOF SYMBOLS AND ABBREVIATIONS

1D	One dimensional
3D	Three dimensional
DC	Damping curve
EL	Equivalent linear
EVP	Elasto-viscoplastic
FFT	Fast fourier transform
MR	Modulus reduction curve
MRD	Modulus reduction and damping
NL	Nonlinear
PGA	Peak ground acceleration

CHAPTER 1 INTRODUCTION

The potential for a site to amplify or attenuate ground motion is usually characterized in practice by either using empirical site factors that depend on average site properties, such as V_{s30} the shear wave velocity in the first 30 meters, or performing ground response analyses to simulate the response of a soil deposit under the vertical propagation of horizontal shear waves. Although more complex, ground response analyses are more accurate because they do not represent average site conditions but are rather site specific, and are slowly becoming standard practice.

The tendency of a site to amplify or attenuate ground motion depends on the soil characteristics, mainly stiffness (G), damping ratio (ξ) and mass density (ρ). There exist three different methods to model the soil behaviour in these analyses: (1) the linear method uses a constant stiffness and damping and considers the soil as linear elastic, (2) the equivalent linear method adjusts shear modulus and damping ratio by using an iterative procedure, (3) the nonlinear method updates the shear modulus and the damping ratio by using a constitutive model based on strain level and loading history. The analyses can be done in time or frequency domain depending on the method used. The linear method uses a frequency domain solution due to the simplicity of calculation. The equivalent linear method also uses the frequency domain during the iterative procedure. The nonlinear method solves the equation of motionin the time domain using constitutive models. The use of the nonlinear method is preferred because it is able to more accurately represent the behaviour of soils under cyclic loading, and it has been shown that it yields better predictions than the equivalent linear and the linear method at strains greater than 0.05 % (Kaklamanos et al. 2015).

Nonlinear site response models for 1D ground response analyses typically use modulus reduction and damping curves as input parameters, and try to approach a perfect match of these input parameters. Models are usually divided into their behaviour during initial loading, defined by a backbone curve, and their behaviour during unloading-reloading, which is controlled by a set of rules. The backbone curve is defined based on the input modulus reduction curve and usually follows a hyperbola formulation. The unload-reload rules depend on the input damping ratio curve, representing the hysteretic behaviour of the soil during unloading reloading. The most elementary rules are the Masing's rules (Masing 1926) where the shape of the unloading-reloading loop is a function of the backbone curve. Since these rules lead to an over prediction of

damping at high strains, they were later modified to match an input damping curve (Hashash and Park 2001, Matasovic and Vucetic 1993, Pyke 2000). Although the modified Masing's rules improve the predictions, theydo not ensure a perfect fit of the damping curve.

1.1 Problematic

Most previous models are unable to match both modulus reduction and damping curves which introduce a misfit of the desired behaviour. Yniesta et al. (2017) proposed a one-dimensional nonlinear stress-strain model, called the ARCS model, able to reproduce any user-input modulus reduction and damping curve. However, soil behaviour is highly strain-rate dependent during monotonic and cyclic loading but none of the above modelsexplicitly include strain rate-dependency. During earthquake loading, the strain rate varies and can reach values up to 100 %/s, a strain rate level that is much higher than classic laboratory tests used to define soil properties. The effect of strain-rate on the behaviour of soils has been studied and for instance, it has been demonstrated that shear strength increases linearly with the logarithm of the strain-rate (Richardson and Whitman (1963), Graham et al. (1983), Lefebvre and LeBoeuf (1987), Kulhawy and Mayne (1990) and Sheahan et al. (1996)), and that damping increases with strain-rate (Darendeli 2001). Afacan et al. (2014) also confirms the strain-rate dependency of shear strength. Isenhower and Stokoe (1981) studied the effect of loading rate on shear modulus and showed that strain-rate influences the latter. Based on the body of literature illustrating the importance of strain-rate, it appears that neglecting to adjust the soil properties to account for strain-rate effects can result in poor predictions (Afacan et al. 2014).

Despite the importance of strain-rate, few models have been developed in order to capture the strain-rate dependency of the soil's cyclic behaviour. For instance Borja (2000) and Mac et al., (2014) proposed elastoviscoplastic models capable of capturing strain-rate effects without controlling damping and modulus behaviour, which is critical in ground response analysis.

Since the nonlinear ARCS model by Yniesta et al. (2017) is able to reproduce any user-input modulus reduction and damping curve, its framework will constitute the basis of a new model that will include strain-rate dependency.

1.2 Objectives

The main objective of this research project is to develop a viscoplastic model for nonlinear 1D ground response analyses capable of capturing strain-rate effects in order to model the dynamic response and capture the strain rate dependence of the soil's behaviour.

This research project aims to achieve the following specific objectives:

- Summarize the viscous features of the soil's response during cyclic loading that have been described in the literature, in particular regarding the strength and the damping behaviour.
- Develop a viscoplastic constitutive model based on the ARCS model that integrates viscous effects observed in the literature such as Sheahan et al. (1996) and Darendeli (2001).
- Implement the viscoplastic model in the ground response analysis software Deepsoil (Hashash et al.2016), by creating a Dynamic Link Library in C++.
- Validate the constitutive model by studying its predictions through a series of ground response simulations modelling a centrifuge tests (Afacan et al. 2014) in Deepsoil in which the results of the analyses and the measurements of the centrifuge are compared in terms surface response spectra.

1.3 Structure of the thesis

This thesis is composed of 6 chapters, including the present one which constitutes an introduction of the 1D dimensional ground response analysis and highlights the problematic and the objectives of this research project. Chapter 2 presents a review of the literature to one dimensional ground response analysis, and is composed of three separate sections. The first section summarizes the theory behind ground response analysis and the different modelling approaches. The second section introduces different nonlinear models and their ability to match or not the input modulus reduction and damping curve. Finally, an introduction to the viscous phenomena that control the mechanical response of soil is presented, along with a few constitutive models including viscous features and their limitations.

Chapter 3 presents the constitutive equations of the proposed viscoplastic model. It first describes the equations of the inviscid part of the model which is based on the ARCS model that permits to match any input damping and modulus reduction curve, before introducing the added viscous stress. The typical predictions of the model are illustrated in Chapter 4 through different examples of single element simulations. For instance, the effects of strain-rate and frequency on the stress-strain response and the hysteretic behaviour are studied. This chapter ends with some discussions regarding the limitations of the viscoplastic model.

Although Chapter 4 illustrates that the model yields the desired general behaviour, it was deemed important to validate the model with full ground response simulations. It is done so in Chapter 5 which first describes the implementation of the viscoplastic model in the ground response analysis software Deepsoil, before showing the performance of the model in such simulations. The latter was studied by comparing the results of 1D ground response analysis and centrifuge tests, in particular the spectral response at the surface of the deposit. When compared to the inviscid model, the proposed viscoplastic model fares better for each motion used in the tests.

Finally, Chapter 6 summarizes the predictive capabilities of the model and the major contributions of this research project. The limitations of the work are discussed and some ideas for potential future work are provided.

CHAPTER 2 REVIEW OF LITERATURE

2.1 One dimensional ground response analysis

Site response analysis consists in simulations studying wave propagation through a soil deposit, and can be performed in one, two or three dimensions. In practice, site response analyses are used to define the potential of a site to amplify or attenuate ground motions and modify the seismic hazard. This study is focusing on 1D ground response analysis, and the integration of viscous effects in such simulations. This section first presents the core concept of ground response simulations, and then presents some of the soil models commonly used in 1D analysis.

A 1D ground response analysis studies the response of a horizontally layered soil deposit, represented by a column, to vertically propagated horizontal shear waves (Figure 2.1). The soil is typically characterized by the shear modulus (G) which defines soil stiffness, the damping ratio (ξ) and the mass density (ρ). Soil behaviour can be represented using different methods explained subsequently. The linear method considers that the soil is linear elastic while the equivalent linear method uses an iterative procedure to adjust shear modulus (G) and damping ratio (ξ) for an equivalent strain to model soil nonlinearities. The nonlinear method uses a constitutive model to update the shear modulus (G) and the damping ratio (ξ) based on the strain level and loading history.

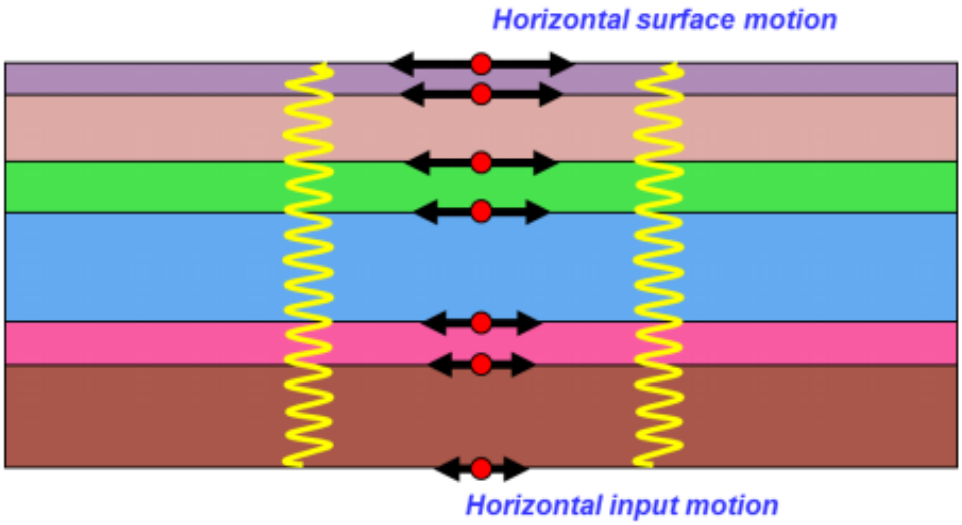

Figure 2.1 Graphical representation of a 1D ground response analysis (J.P. Pruiksma 2016)

In one dimensional ground response analysis, the calculations can be done in time or frequency domain. Time domain solutions calculate the response of the soil at every time step, while frequency domain solutions compute the Fourier spectrum of the soil's response based on the input motion and transfer functions computed with the theory of continuum mechanics. Whether time or frequency domain solutions can be used depends on the method used to model the soil behaviour, either the linear method, the equivalent linear (EL) method or the nonlinear (NL) method. The methods are described briefly in the subsequent sections.

2.2 Linear analysis

The linear method considers that the soil is linear elastic and uses a constant damping ratio ξ and a constant shear modulus, which can be calculated with the following equation :

$$G_{max} = \rho \, . V_s^{\,2} \qquad \text{Equation 2.1}$$

where ρ is the soil density and V_s the shear wave velocity. Linear analyses are well suited for a frequency domain solution because the transfer functions are easy to compute and provide an exact solution. However, the assumption that the soil would behave as a purely elastic medium during wave propagation is known to be incorrect (Kaklamanos et al. 2015).

2.3 Equivalent linear analysis

The equivalent linear method (EL) (Seed and Idriss (1969)) uses an iterative procedure typically performed in the frequency domain to solve the wave propagation problem and introduces a degree of nonlinearity in the soil's behaviour. It requires the following input parameters:

- soil density (ρ);
- maximum shear modulus (G_{max});
- a modulus reduction curve that represents the decrease of stiffness of the soil when shear strain increases;
- a damping ratio curve $\xi(\gamma)$ that represents the increasing capacity of the soil to dissipate hysteretic energy upon cyclic loading when cyclic shear strain increases.

In the equivalent-linear formulation, the values of G and ξ of each soil layer are iteratively adjusted to be consistent with the effective level of shear strain. For earthquake input motions, in

a given layer, Seed and Idriss (1969) suggested to calculate the properties for an equivalent strain equal to 2/3 of the maximum strain level.

The iterative procedure for the equivalent linear model is stated as follows:

1) Assign initial parameters;
2) Perform a linear shear wave propagation analysis;
3) Calculate the maximum strain in every layer;
4) Calculate the effective shear strain γ_{eff} equal to 2/3 of the maximum strain;
5) Re-calculate new pair of G and ξ based on the new strain level;
6) Repeat the procedure until the maximum strain for all layers converge for two consecutive calculations.

Due to its simplicity, the EL method was the most used in both research and engineering practice, but it does have some limitations. In an EL simulation, the properties are assumed to remain constant throughout the entire simulation, whereas, in reality, the shear modulus and damping ratio vary during the wave propagation. This assumption sometimes leads to cases where the equivalent linear method does not represent the behaviour of the soil column and yields unrealistic results, in particular at high strains (Kaklamanos et al. 2013, Stewart et al. 2008). For instance, when the soil layer deforms significantly ($\gamma > 0.05\%$), the equivalent linear method gives poor predictions (Kaklamanos et al. 2015). In this case, a nonlinear analysis is preferred to represent the variation of the shear modulus (G) and the damping ratio (ξ) with strain.

2.4 Nonlinear analysis

2.4.1 Definition of nonlinear analysis

In a nonlinear analysis, the soil column is divided into individual layers using either a multi-degree-of-freedom lumped mass model or finite elements. Figure 2.2 presents a schematic representation of these two approaches.

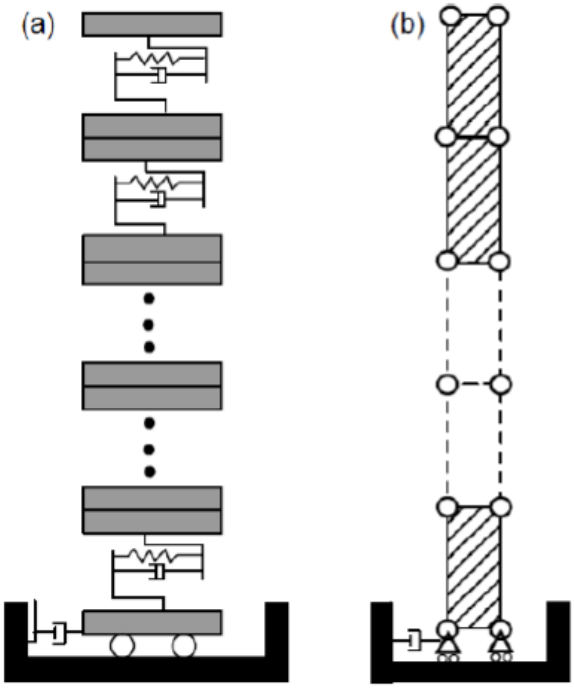

Figure 2.2 Representation of Soil Column (a) Lumped Mass System (b) Distributed Mass (Stewart et al. 2008)

In the lumped mass model, each individual layer is represented by a corresponding mass, nonlinear spring, and a dashpot. In a finite element simulation, every layer is subdivided into small elements that have distributed mass. Stiffness, damping and mass matrix are assembled differently depending on the approach chosen. Theoretically, although the calculations are different, the two approaches should lead to similar results.

Nonlinear analyses are always performed in the time domain where the following dynamic equation of motion is solved at every time step:

$$[M]\{\ddot{u}\} + [C]\{\dot{u}\} + [K]\{u\} = -[M]\{I\}\,\ddot{u}_g \qquad \text{Equation 2.2}$$

where *[M]* is the mass matrix, *[C]*is the damping matrix, *[K]* is the stiffness matrix, $\{\ddot{u}\}$ is the vector of nodal relative accelerations, $\{\dot{u}\}$ is the vector of nodal velocities, $\{u\}$ is the vector of nodal displacements, $\ddot{u}_g$ is the acceleration at the base of the soil column and *{I}* is the unit vector. At every time step, Equation 2.2 is solved using a time integration method (e.g.

Newmark β method (1959)), and the damping and stiffness matrices are updated based on the soil's constitutive model.

Many constitutive models have been developed in order to describe the cyclic behaviour of soil in 1D ground response analysis. To do so, most models use modulus reduction and damping curves as input parameters and define the stress-strain behaviour based on these input curves. The modulus reduction curve defines the backbone stress strain curve that describes the response of soil during initial loading. The damping ratio curve defines the hysteretic behaviour of the soil during unloading-reloading based on a set of rules.

One-dimensional models are evaluated by analyzing their ability to match their input modulus reduction and damping curves. When a model fails to match its input curves, it introduces a misfit of the desired behaviour. Note that as a result of the rules and the model's assumptions, G and ξ vary throughout the duration of loading when performing fully nonlinear analyses.

2.4.2 Empirical relationships for modulus reduction and damping

As previously mentioned, most constitutive models used in one-dimensional ground response use modulus reduction and damping curves as inputs parameters and the ability of a model to match the input curves defines how good the model is. To measure the modulus reduction and damping curves, laboratory tests are required through the use of advanced devices such as resonant column or direct simple shear tests. In most projects, such devices are either unavailable or too expensive to be used, and empirical relationships are used in order to calculate the modulus reduction and the damping curves.

Darendeli (2001) introduced empirical relationships to calculate modulus reduction and damping curves of clays based on the plasticity index (*PI*), the overconsolidation ratio (*OCR*), and the mean effective stress (σ'_0). Darendeli's equations are not able to predict the response of soils at large strains because Darendeli's equations were derived based on lab tests where strains rarely reached more than 0.3% (Figure 2.3). Despite their shortcomings, Darendeli's equations are widely used in practice.

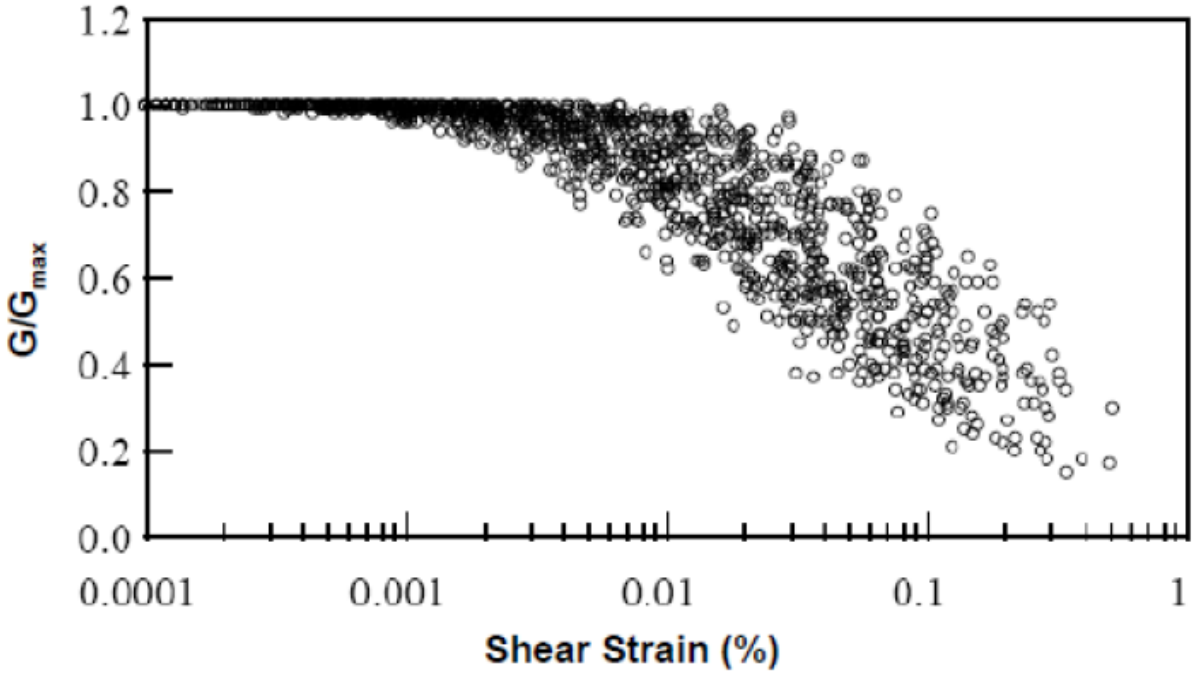

Figure 2.3 Darendeli's database (Darendeli 2001)

Based on Darendeli's work, Menq (2003) introduced modulus reduction and damping relationships for granular soils based on mean effective stress (σ'_0), coefficient of uniformity (C_u) and mean grain size (D_{50}).

Once the modulus reduction and the damping curves are defined for every soil layer, they are used as input parameters in order to describe the cycle behaviour of soil during initial loading and unloading-reloading. The following sections describe how models try to match these input parameters and the difficulties encountered.

2.4.2.1 Initial loading

During initial loading, the stress-strain behaviour of the soil is defined by a backbone curve, which can directly be calculated from the modulus reduction curve. The backbone curve is usually modeled with a hyperbola (Hardin and Drnevitch (1972)). If the desired modulus reduction curve is hyperbolic, then the nonlinear codes using a hyperbolic equation to model the backbone curve will precisely match the desired modulus reduction curve. However, when the target modulus reduction curve is not a hyperbolic function, this formulation introduces a misfit between the input modulus reduction curve and the hyperbolic curve. In particular, small misfits

in the modulus reduction curve can lead to important misfits of the stress-strain curve at high strains, rendering an unrealistic shear strength leading to inaccurate estimates of site response.

Several solutions have been proposed to palliate the shortcomings of the hyperbolic model. For instance, Hashash et al. (2010) proposed to adjust the high strain part of the user-input modulus reduction curve so the shear strength resulting from the fitted curve is correct. However, this method increases the misfit at low strains. Yee et al (2013) proposed to modify the modulus reduction curve to match the shear strength at high strains, the obtained backbone curve is then more reasonable and does not present a misfit at low strains. However, the model cannot be adjusted perfectly by a hyperbolic model, which often results in a difference between the desired shear strength and the one obtained in the nonlinear response code of the site. Groholski et al. (2016) introduced a General Quadratic/Hyperbolic (GQ/H) model which allows to match an input target strength and also to match precisely an input modulus reduction curve at low and large strains. This model satisfyingly solves the problem of matching the shear strength without modifying the low strain behaviour of the stress-strain curve.

2.4.2.2 Unloading-reloading rules

Masing (1926) rules and extended Masing rules are a set of rules that describe the one dimensional nonlinear cyclic soil behaviour. The extended Masing rules are described below.

1. During initial loading, the stress-strain behaviour of soil follows the backbone curve.
2. After a change of loading direction, the unloading or reloading curve follows the backbone curve enlarged by a factor *n*. Masing defined the factor *n* equal to 2, but it was modified by Pyke (1979) in order to obtain a better fit of the damping curve at high strains.
3. When the maximum past strain is exceeded during unloading or reloading, and if the stress-strain curve intersects the backbone curve, it follows the backbone curve until the next change of direction.
4. If the unloading or reloading curve crosses a previous cycle of unloading or reloading curve, the stress-strain curve follows the curve of this previous cycle.

Masing rules are known to have a tendency of over predicting damping at large strains (Phillips and Hashash 2009). To obtain a correct hysteretic damping at high strains, several solutions have

been proposed to modify one or several of Masing rules. Cundall-Pyke (Pyke 1979) evaluated the factor *n* based on the shear strength to obtain abetter match of the damping at large strains, however, this method introduces some degradation. Darendeli (2001) introduced a damping reduction factor that modifies the area inside the stress-strain curve in order to improve the match of the input damping curve. Based on this study, Phillips and Hashash (2009) introduced a damping reduction factor that gave a better match of the curve at higher strains.

On the other hand, Masing rules do not introduce hysteretic damping at low strains where the backbone curve is linear. In order to introduce small-strain damping, nonlinear codes relies on frequency dependent Rayleigh damping (Rayleigh and Lindsay 1945) in which the damping matrix *[C]* results from a combination of two matrices, the first is proportional to the mass matrix *[M]* and the second is proportional to the stiffness matrix *[K]* as shown in the following equation:

$$[C] = a.[M] + b.[K] \qquad \text{Equation 2.3}$$

where a and b are scalar values selected to obtain a given damping value for two control frequencies. There exist several damping schemes that match a different number of control frequencies. For instance full Rayleigh damping and extended Rayleigh damping match 2 and 4 frequencies respectively (Rayleigh and Lindsay (1945), Park and Hashash (2004)). Figure 2.4 presents a comparison of the effective damping obtained using Rayleigh damping and extended Rayleigh with different frequencies matched (one mode, two modes and four modes solutions).

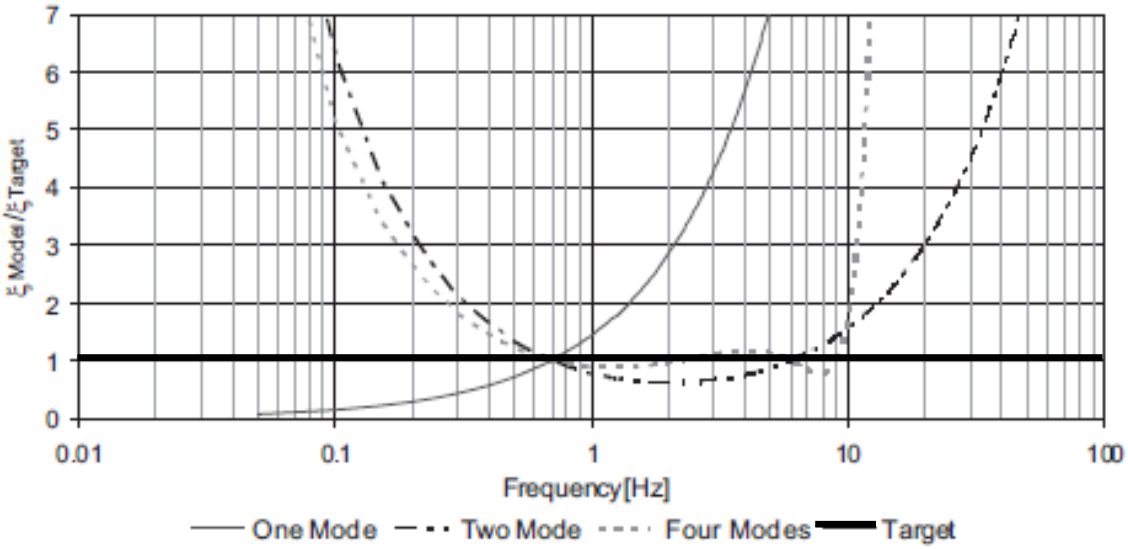

Figure 2.4 Effective damping for one, two and four modes frequency dependent Rayleigh damping (Phillips and Hashash 2009)

The frequency dependence arising from Rayleigh damping is inconsistent with available experimental results (Vucetic et al. 1998) which mean that material damping in soils is frequency independent at very small strain levels. Moreover, the small-strain damping is only consistent with the target damping at the control frequencies and either overestimates or underestimates the target damping at other frequencies. Phillips and Hashash (2009) established a frequency-independent Rayleigh damping formulation to match the small strain damping. The formulation was based on the work of Liu and Gorman (1995) and provides a realistic damping by reducing the over-damping at both high and low frequencies.

Yniesta et al. (2017) proposed a one-dimensional nonlinear stress-strain model able to reproduce any user-input modulus reduction and damping curve that includes hysteretic damping even at small strains by departing from the Masing rules. This model, presented in this document, is based on the formulation from Yniesta et al. (2017), and will be extensively presented in Chapter 3.

2.5 Viscoplasticity and viscoelasticity

None of the nonlinear models mentioned above include strain rate-dependency. However, several studies (Sheahan et al. (1996), Darendeli (2001)) have shown that soil behaviour is highly strain-rate dependent during both monotonic and cyclic loading. In this context, few models have been

developed for cyclic loading in order to capture the strain rate dependency of the soil's behaviour. This section defines the viscous phenomena observed in the soil's behaviour, before introducing different types of time-dependent models and their limitations.

2.5.1 Viscous phenomena

2.5.1.1 Creep

Creep is the slow continuous deformation of a material under constant stress. At point A (Figure 2.5), the stress is fixed and as time progresses, the strain increases and moves to point B. The continuous increase of strain without a change in stress is defined as creep.

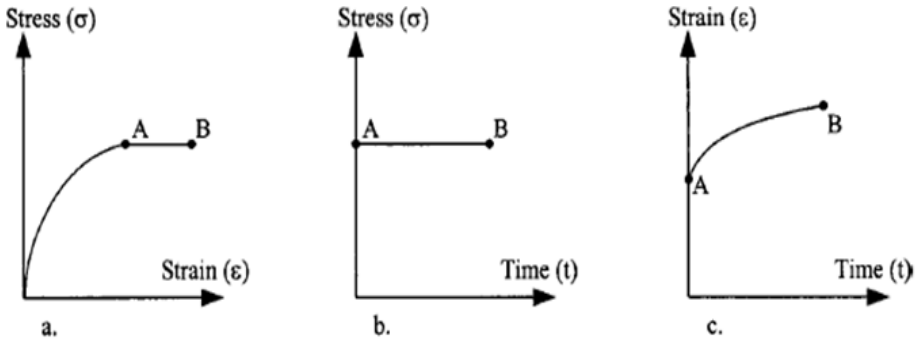

Figure 2.5 Creep test (a) Stress-strain curve (b) Stress history (c) Strain history (Augustesen et al. 2004)

2.5.1.2 Relaxation

A stress relaxation test is illustrated in Figure 2.6. At point A, the total strain is fixed and as time progresses, the stress–strain state moves to point B. During this process, the stress is gradually decreasing, it relaxes.

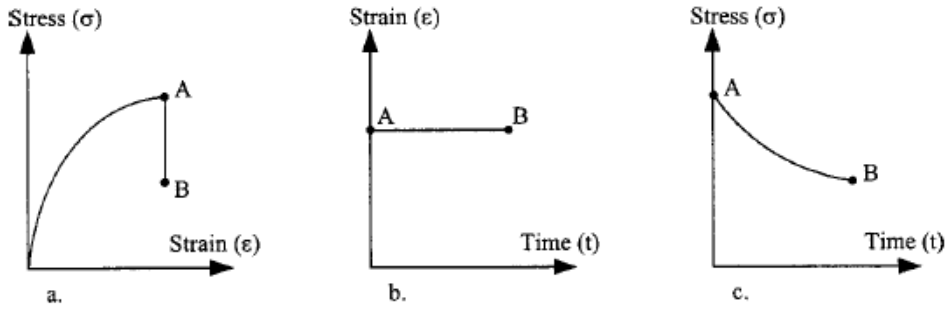

Figure 2.6 Relaxation test (a) Stress-strain curve (b) Stress history (c) Strain history (Augustesen et al. 2004)

2.5.1.3 Strain-rate effects

Several studies have observed that shear strength generally increases with the increase of strain rate (Richardson and Whitman (1963), Graham et al. (1983), Lefebvre and LeBoeuf (1987), Kulhawy and Mayne (1990) and Sheahan et al. (1996)). Based on the results of undrained triaxial tests on clays, Sheahan et al. (1996) postulated that the shear strength increases linearly with the logarithm of the strain rate, and that the increase varies between 5 % and 20 % per logarithmic cycle of strain rate (Figure 2.7).

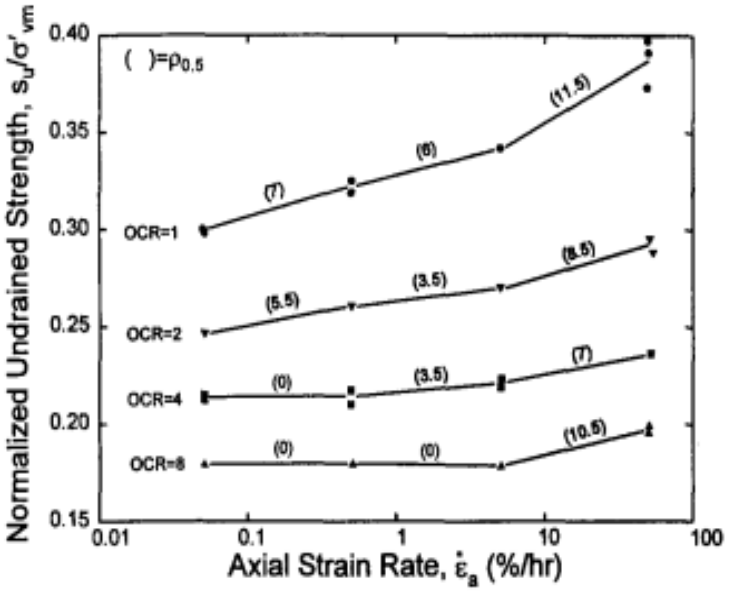

Figure 2.7 Shear strength increase per strain rate (Sheahan et al. 1996)

Darendeli (2001) studied the effect of strain rate on damping by studying the effect of loading frequency on the results of cyclic laboratory tests. He deduced that damping increases with loading frequency (Figure 2.8) i.e. with strain rate.

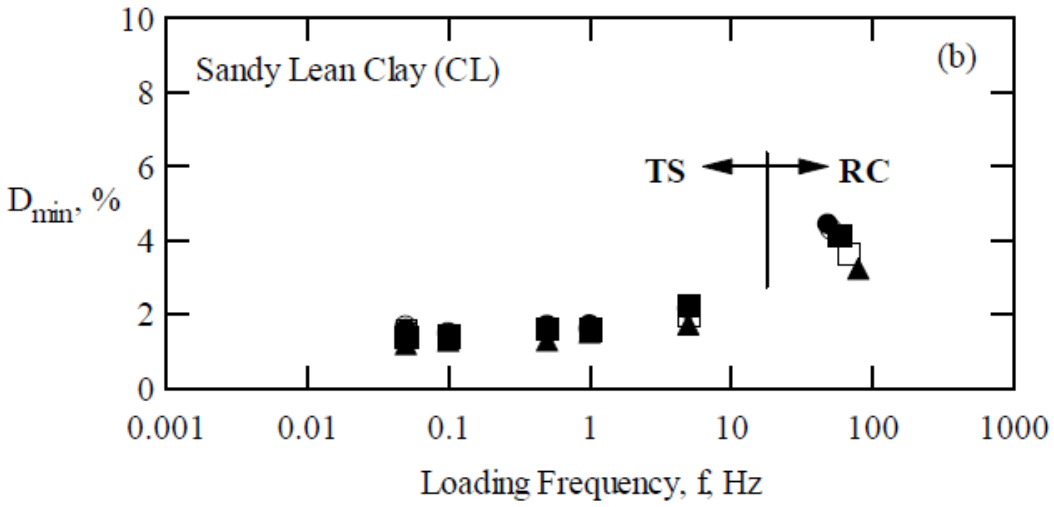

Figure 2.8 Effect of loading frequency on small strain damping (Darendeli 2001)

2.5.2 Time-dependent models

The strain rate dependency of the soil's behaviour is supposed to be related to viscous effects discussed in the previous section (creep, stress relaxation, and strain-rate effects). To capture these effects, several constitutive models have been developed in order to obtain realistic solutions for time-dependent engineering problems, but their use in site response analysis remains marginal. Liingaardet al. (2004) categorized the models dealing with time dependent behaviour of soil into three major types: empirical models, rheological models and general stress-strain time models.

2.5.2.1 Empirical models

These models are rate-dependent constitutive models which formulations do not rely on physics but rather on empirical equations. The parameters for the equations can be obtained by directly adjusting test results of creep, stress relaxation, and constant strain rate. For example, Yin (1999), based on tests results, presented a function that describes the creep behaviour as a function of time. Empirical models can also be obtained by combining other empirical models. Yin and

Graham (1994, 1996) developed a series of time-dependent models that describe creep behaviour of clays by integrating an “equivalent time” parameter that depends on time. The application of these models is mostly limited to boundary conditions. In addition, these models do not work for cyclic loading since they do not describe the cyclic behaviour of soil.

2.5.2.2 Rheological models

Rheological models were first developed in order to describe the behaviour of metals and later modified to be applied for soils. In the case of metals, the models mostly represent a viscous or time-dependent behaviour. In the case of soil, they can also represent the plastic behaviour. There are several categories of approach for rheological models. For instance, the differential approach consists in combining different models of elementary materials with springs and dashpots. For example, the Maxwell model consists in combining a spring and a dashpot in series, Kelvin–Voigt model consists in combining a spring and a dashpotin parallel. A second approach used is the hereditary approach which allows to obtain the strain by integration over the entire loading history. The main limitation of these models is that theydo not work for cyclic loading. For more details, readers are referred to Liingaardet al. (2004).

2.5.2.3 General stress-strain time models

General stress–strain-time models are multi-dimensional models that describe both the viscous and the inviscid soil behaviour. It includes a variety of models (inviscid models, elastoviscoplastic models (EVP) and viscoelastic-viscoplastic models). The EVP models are the most widely used one (e.g. Kutter and Sathialingam (1992), Yin and Graham (1999)). They integrate the time-dependent stress-strain behaviour of soil by introducing a time-dependent yield function and divide the strain-rate tensor into an elastic-strain-rate tensor and a viscoplastic-strain-rate tensor. Most existing models are based either on the Perzyna (1966) or the Duvaut-Lion (1972) formulations, with the latter being an extension of the former.

General stress–strain-time models can be used for cyclic loading but do not control modulus and damping curve. In addition, these models are mathematically complex and require input parameters that are not physically meaningful, and often hard to calibrate. A few of these models are shortly described in the following section.

2.5.2.3.1 N. Mac, B. Shahbodaghkhan and N. Khalili. (2014)

N. Mac, B. Shahbodaghkhan and N. Khalili. (2014) proposed an elastic-viscoplastic (EVP) constitutive model for the analysis of time-dependent behaviour of clay. The constitutive model is based on the bounding surface plasticity and allows a transition from elastoplasticity to viscoplasticity. The rate-dependent bounding surface introduces viscous effects whether the stress state is on or inside the bounding surface. The total strain increment is then decomposed into elastic part and viscoplastic part.

Figure 2.9 presents a comparison between experimental data and the model's predictions for triaxial compression tests performed at two different strain rates. The results showed an increase of stiffness and strength with the increase of strain rate consistent with the experimental data.

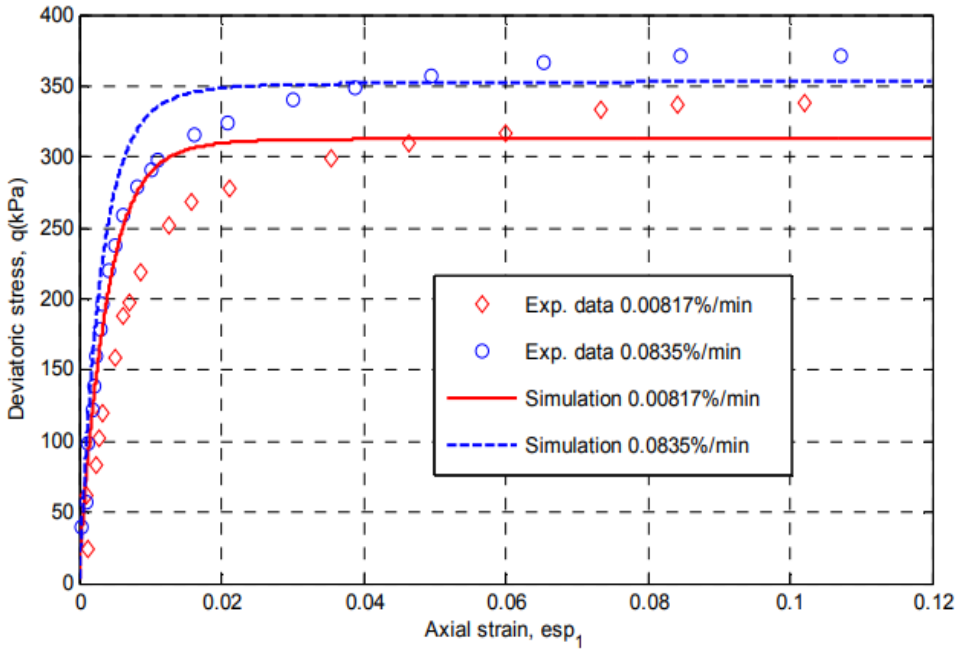

Figure 2.9 Effect of strain rate on the stress-strain response (N. Mac, B.Shahbodaghkhan, & N. Khalili. 2014)

Although the model is able to capture some viscous features of the soil's behaviour, such as the strength and stiffness increase, the proposed constitutive model does not control the damping nor the modulus reduction curve during cyclic loading.

2.5.2.3.2 Borja et al. (2000)

Borja et al. (2000) presented an elasto-plastic constitutive model for non-liquefiable soils. The model is based on bounding surface plasticity with an elastic region that moves and translates inside a bounding surface. Shear strength variation are captured thanks to the translation of the bounding surface in the stress space. The stress is divided into inviscid and viscous parts:

$$\sigma = \sigma^{inv} + \sigma^{vis} \qquad \text{Equation 2.4}$$

Where σ^{inv} is the inviscid stress and σ^{vis} the viscous stress. The latter depends on a strain rate vector$\dot{\varepsilon}$ and a viscous damping parameter *D* calculated based on ξ_0, the value of damping ratio in the limit of zero shear strain, $\omega$the angular frequency and c^e the elastic tensor module.

$$\sigma = \sigma^{inv} + D.\dot{\varepsilon} \qquad \text{Equation 2.5}$$

$$\sigma = \sigma^{inv} + \frac{2\xi_0}{\omega} c^e.\dot{\varepsilon} \qquad \text{Equation 2.6}$$

The added viscous stress allows to capture strain-rate effects. For instance, a rounded tip of the stress-strain curve is obtained upon a change of direction (Figure 2.10) which is consistent with the behaviour observed in cyclic tests under sinusoidal loading (Vucetic et al. 1998).

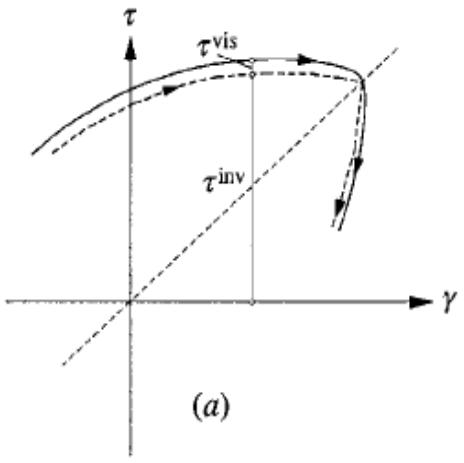

Figure 2.10 Effect of viscous stress on the stress-strain curve (Borja et al. 2000)

The model is capable of capturing strain rate effects on the shear strength and can be used for cyclic loading. However, only the damping ratio value at the limit of zero shear strain is

specified, rather than the entire damping ratio curve, so the model does not control the damping nor the modulus reduction curve.

2.5.2.3.3 Kutter and N. Sathialingam (1992)

Kutter and N. Sathialingam developed a constitutive model in order to capture the strain rate-dependency of clays. The model is based on the elastic-viscoplasticity theory previously discussed where the inelastic strains are considered viscoplastic. The constitutive model focuses on the prediction of the primary and secondary compression rather than cyclic loading. The coefficient of secondary compression C_α measured during compression tests allows to introduce strain-rate effects. It has been demonstrated that the strain rate effecton undrained shear strength of a soil can be predicted based on this coefficient (Figure 2.11), with soils with higher C_α having greater shear strength increase per logarithm cycles of strain rate.

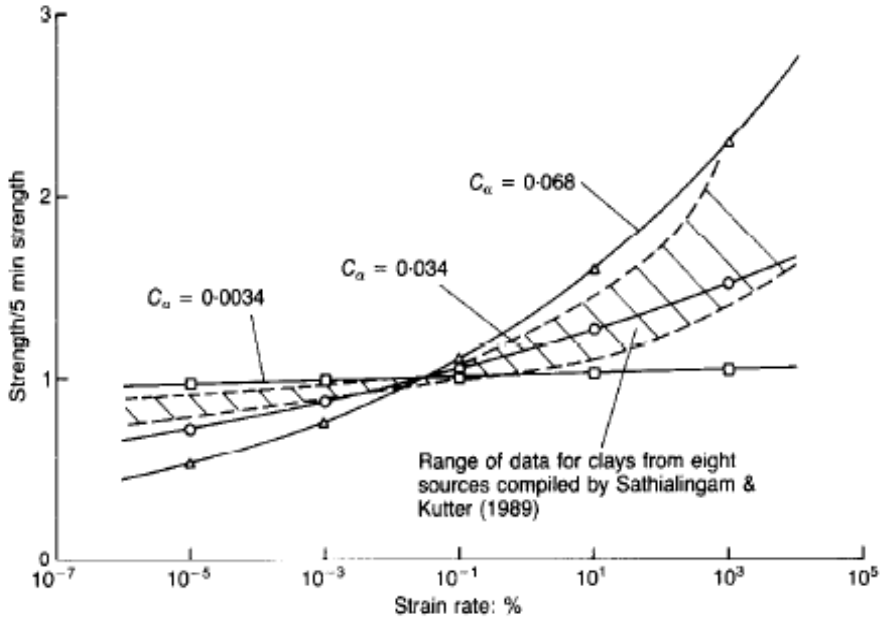

Figure 2.11 Effect of strain rate on shear strength (Kutter and N. Sathialingam (1992))

A comparison between the predictions of the model and the results of undrained triaxial compression tests performed at different strain-rates has been done (Figure 2.12). The model is able to capture the increase in deviatoric stress observed with an increase of strain rate.

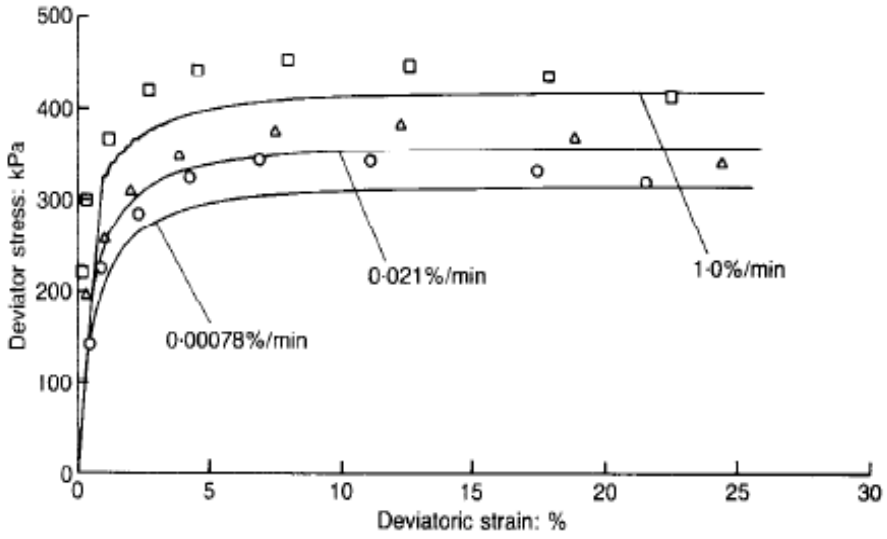

Figure 2.12 Effect of strain-rate on stress-strain response (Kutter and N. Sathialingam (1992))

This model is well-suited to describe the monotonic behaviour of the soil under a variety of stress-path. However, the model's input parameters pertain only to the monotonic behaviour of the soil, and the model's predictive capabilities have not been studied for cyclic applications. Therefore the model would not control modulus reduction and damping response, but it is expected, based on the formulation of the constitutive equations, that the model would overpredict damping at large strains.

CHAPTER 3 FORMULATION OF A VISCOPLASTIC MODEL FOR NONLINEAR 1D GROUND RESPONSE ANALYSES

3.1 Introduction

Nonlinear one-dimensional ground response analyses are performed using a constitutive model that controls the response of soil elements to seismic loading. Such models are formulated to return a shear stress (τ) as a function of a new shear strain (γ). As presented in the previous chapter, existing models use a modulus reduction and a damping curve (MRD) as input parameters, and do not consider viscous effects. The accuracy of a model and its predictive capabilities in ground response analysis is defined by its ability to match the target curves. For instance, a poor fit of the modulus reduction curve can cause an under or over prediction of shear strength which can lead to under or over prediction of ground surface motion. Yniesta et al. (2017) presented a one-dimensional nonlinear stress-strain model (ARCS model) able to reproduce any user-input modulus reduction and damping curve. This model follows the theoretical framework of rate-independent plasticity, however, soil behaviour is highly strain-rate dependent during monotonic and cyclic loading. Thus, it is essential to capture the strain rate dependence of the soil's behaviour.

This chapter presents the constitutive equations of a viscoplastic model capable of capturing the strain rate dependency of soils. The model is based on the ARCS model that permits to match any input damping and modulus reduction curve and is divided into viscous and inviscid parts following the work from Borja et al. (2000).

$$\tau = \tau_{inv} + \tau_{visc} \qquad \text{Equation 3.1}$$

Where τ_{inv} and τ_{visc} are the inviscid and viscous stresses respectively.

3.2 Inviscid stress

The inviscid part of the model is based on the formulation of the ARCS model (Yniesta et al. 2017) briefly presented below. For more details the reader is referred to the original publication.

3.2.1 Backbone curve

During initial loading, the ARCS model follows the backbone curve as defined by the input modulus reduction curve, by using a cubic spline fit. This type of interpolation fits cubic splines through all of the data points which allows to correspond to any modulus reduction curve. This formulation has been compared to two different approaches of ahyperbolic fit: hyperbolic fit of the modulus reduction and hyperbolic fit of the backbone (Figure 3.1)

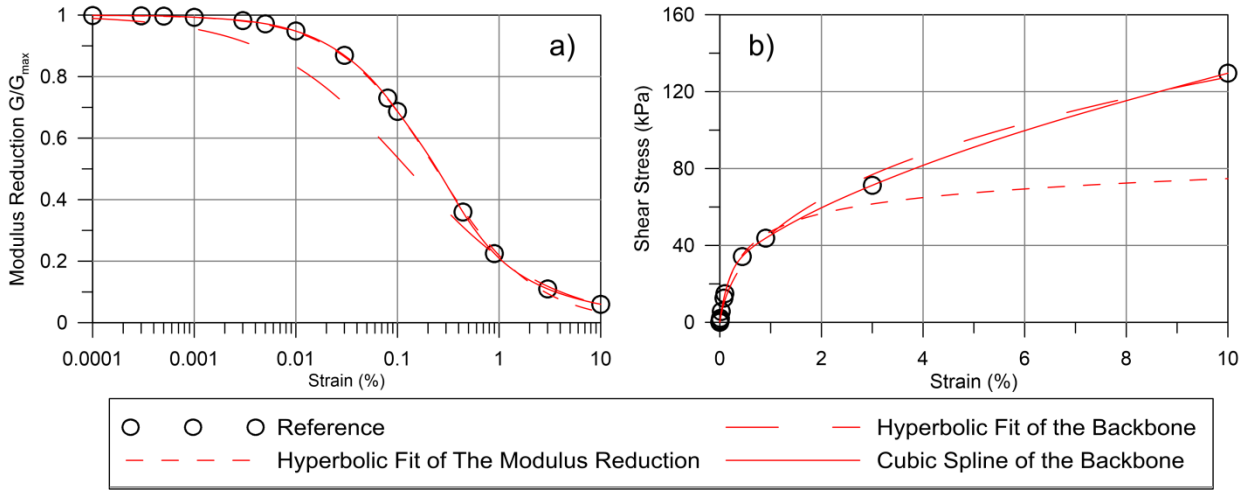

Figure 3.1 Comparison of the curve fitting method on (a) the modulus reduction curve and (b) the backbone curve (Yniesta et al. (2017))

The hyperbolic fit of the modulus reduction fits the modulus reduction curve but results on a slight misfit at high strains in the backbone curve thatleads to an under-prediction of shear strength. The hyperbolic fit of the backbone fits the backbone curve and matches the target strength but results on a misfit on the modulus reduction curve at small strains. These evaluations confirm thatthe cubic splineinterpolation is well-suited to match a target modulus reduction curve.

3.2.2 Unload-reload rules

The unload-reload rules are formulated in order to meet the following criteria:

(i) the model matches any user-input modulus reduction curve;

(ii) when the cyclic strain input is uniform, the stress-strain curve close and repeat without cyclic degradation or stiffening;

(iii) the area inside the stress-strain curve is consistent with the user-input damping curve even at small strains;

(iv) the stress-strain loops are concave about the secant modulus line.

3.2.2.1 Rotation of the coordinate system

Yniesta et al. (2017) unload-reload rules use a coordinate transformation approach to calculate the shear stress. Upon unloading or reloading, a new coordinate system is defined based on target (γ_R,τ_R) and previous (γ_L,τ_L) reversal stress-strain points that are defined from the loading history. Note that the target and previous reversal stresses are inviscid, as are all the stresses defined in this section. An axis γ' that runs through the target and the previous stress-strain points is defined (Figure 3.2) it has an angle θ from the γ axis. The τ' axis is orthogonal to γ', and the center of (γ_L,τ_L) and (γ_R,τ_R) represents the origin of the new coordinate system (γ_0,τ_0).

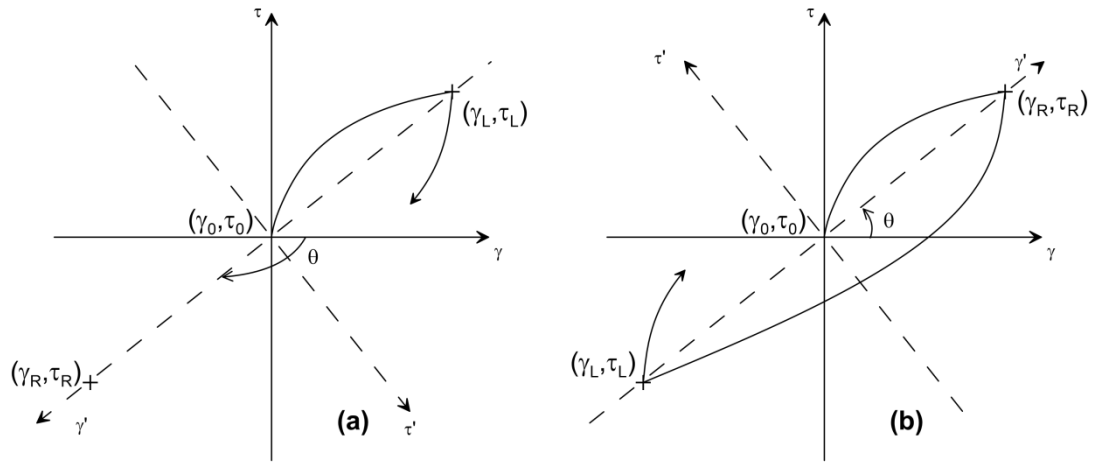

Figure 3.2 Stress-strain loops during (a) unloading and (b) reloading (Yniesta et al. 2017)

The orientation θ of the new coordinate system is defined based on the loading direction, which is positive if the strain increment $d\gamma$ is positive (case (a)) and negative if $d\gamma$ is negative (case (b)):

$$\theta = tan^{-1}\left(\frac{\tau_R-\tau_L}{\gamma_R-\gamma_L}\right) \quad \text{case(a)} \qquad \text{Equation 3.2}$$

$$\theta = tan^{-1}\left(\frac{\tau_R-\tau_L}{\gamma_R-\gamma_L}\right) - \pi \quad \text{case(b)} \qquad \text{Equation 3.3}$$

In the new coordinate system, the current stress-strain pointhas the following coordinates (γ',τ'):

$$\begin{pmatrix}\gamma'\\ \tau'\end{pmatrix} = \begin{pmatrix}(\gamma-\gamma_0)\cos\theta + (\tau_{inv}-\tau_0)\sin\theta\\ -(\gamma-\gamma_0)\sin\theta + (\tau_{inv}-\tau_0)\cos\theta\end{pmatrix} \quad \text{Equation 3.4}$$

Any set of transformed coordinates can be expressed in the original system (γ,τ_{inv}) as follows:

$$\begin{pmatrix}\gamma\\ \tau_{inv}\end{pmatrix} = \begin{pmatrix}\gamma'\cos\theta - \tau'\sin\theta + \gamma_0\\ \gamma'\sin\theta - \tau'\cos\theta + \tau_0\end{pmatrix} \quad \text{Equation 3.5}$$

3.2.2.2 Stress-strain curve in rotated coordinate space

In the transformed coordinate system, the stress strain curve follows a biquadratic equation defined as follows:

$$\tau' = a\gamma'^4 + b\gamma'^2 + c \quad \text{Equation 3.6}$$

In the transformed coordinate system, the target reversal strain γ'_{in} defines the shape of the loop (Figure 3.3). γ'_{in} is defined by:

$$\gamma'_{in} = \frac{(\gamma_R - \gamma_L)}{\cos\theta} \quad \text{Equation 3.7}$$

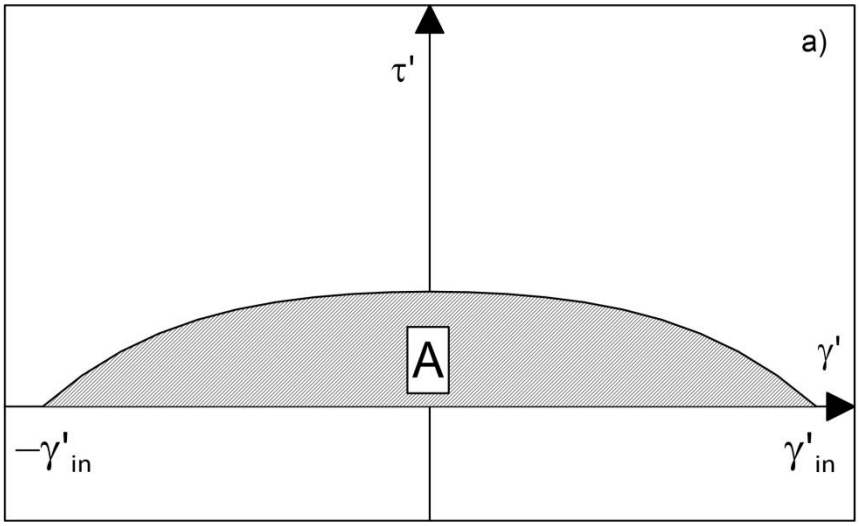

Figure 3.3 Half stress-strain loop in the transformed coordinate system (Yniesta et al.2017)

To satisfy criterion (ii) which requires that the unload-reload loops close without any cyclic degradation or hardening, the following equation must be applied:

$$\tau'(\gamma'_{in}) = 0 \quad \text{Equation 3.8}$$

In order to satisfy criterion (iii) requiring that the area inside the loop match a target damping value, the following equation is used:

$$\int_{-\gamma'_{in}}^{\gamma'_{in}} \tau'(\gamma')d\gamma' = A = \gamma'_{in} D\pi(\tau_R - \tau_0)cos\theta \qquad \text{Equation 3.9}$$

where A is the area below half of the loop, and D is the equivalent viscous damping ratio selected from the input damping ratio curve based on the cyclic strain amplitude γ_c:

$$\gamma_c = \frac{|\gamma_R - \gamma_L|}{2} \qquad \text{Equation 3.10}$$

The previous equation relies on the definition of the hysteretic damping ratio:

$$D = \frac{2A}{4\pi B} \qquad \text{Equation 3.11}$$

where B is the area of the triangle shown on Figure 3.4.

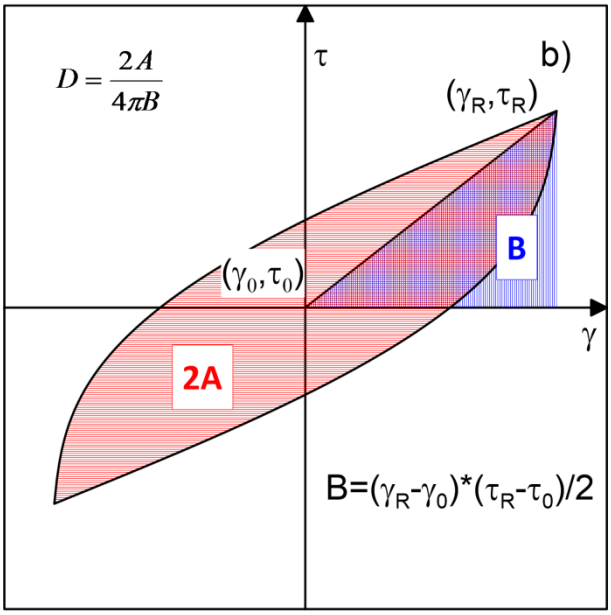

Figure 3.4 Definition of damping (Yniesta et al.2017)

To satisfy criterion (iv), requiring that the stress-strain curve to be concave about the secant shear modulus line, the following formulation is satisfied:

$$\frac{d^2(\tau')}{d(\gamma')^2} \leq 0$$ Equation 3.12

Note that the last criterion is a consequence of the functional form chosen for the stress-strain curve in order to yield realistic stress-strain curves. The system of equations formed by Equation 3.8, Equation 3.9 and Equation 3.12 can be solved to define the coefficients *a*, *b*, and *c*:

$$a = \frac{5\pi D cos\theta(\tau_R - \tau_0)}{32{\gamma'}_{in}^{4}}$$ Equation 3.13

$$b = -\frac{15\pi D cos\theta(\tau_R - \tau_0)}{16{\gamma'}_{in}^{2}}$$ Equation 3.14

$$c = \frac{25\pi D cos\theta(\tau_R - \tau_0)}{32}$$ Equation 3.15

Substituting Equation 3.6 in Equation3.8, Equation 3.9, Equation 3.12 results in an equation that calculates the new inviscid stress:

$$\begin{aligned}\tau_{inv} = {} & [(\gamma - \gamma_0)\cos\theta + (\tau_{inv} - \tau_0)\sin\theta]\sin\theta \\ & + [a((\gamma - \gamma_0)\cos\theta + (\tau_{inv} - \tau_0)\sin\theta)^4 \\ & + b((\gamma - \gamma_0)\cos\theta + (\tau_{inv} - \tau_0)\sin\theta)^2 + c]\cos\theta + \tau_0\end{aligned}$$ Equation 3.16

In the final equation obtained, the new inviscid stress τ_{inv} is the sole unknown. The equation can be solved using Ridder's Method (Ridder 1979), a root-finding algorithm based on the false position method. The two initial roots are set as the inviscid stress at the previous time step and the target inviscid stress since they both lie on different sides of the root being sought.

3.2.2.3 Asymmetrical loading

Asymmetrical loading conditions happen when (γ_R,τ_R) ≠ (-γ_R,-τ_R). The origin of the coordinate transformation is no longer identical to τ-γ origin (Figure 3.5).

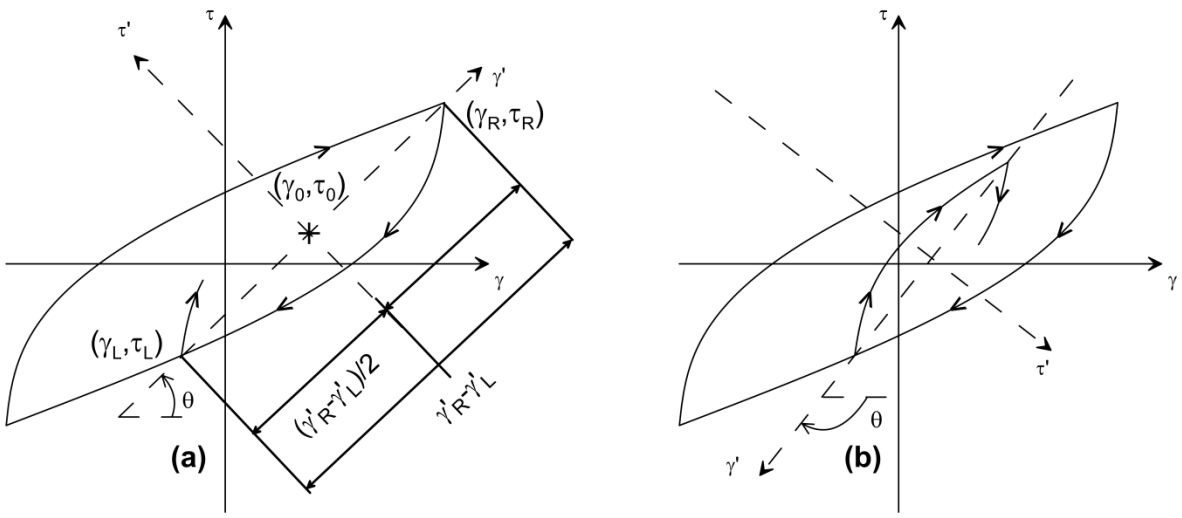

Figure 3.5 Asymmetrical loading (a) positive loading (b) negative loading (Yniesta et al.2017)

The model keeps track of the values of shear stress and strain at each reversal of loading, and selects the target and previous reversal points from the reversal points based on three rules.

(1) When unloading happens after initial loading, the previous reversal point is defined as the unloading point and the target point is defined as the symmetrical point (Figure 3.6 case (a)).

(2) Upon a change of loading direction from an existing unload/reload loop, the reversal point is defined as the previous reversal point, and the previous reversal point of the initial unload/reload loop becomes the target reversal point (Figure 3.6 case (b)).

(3) When a reloading cycle exceeds the target strain γ_R, the current values of γ_L and γ_R are deleted, and the previous values of γ_L and γ_R are reinstated (Figure 3.6 case (e)).

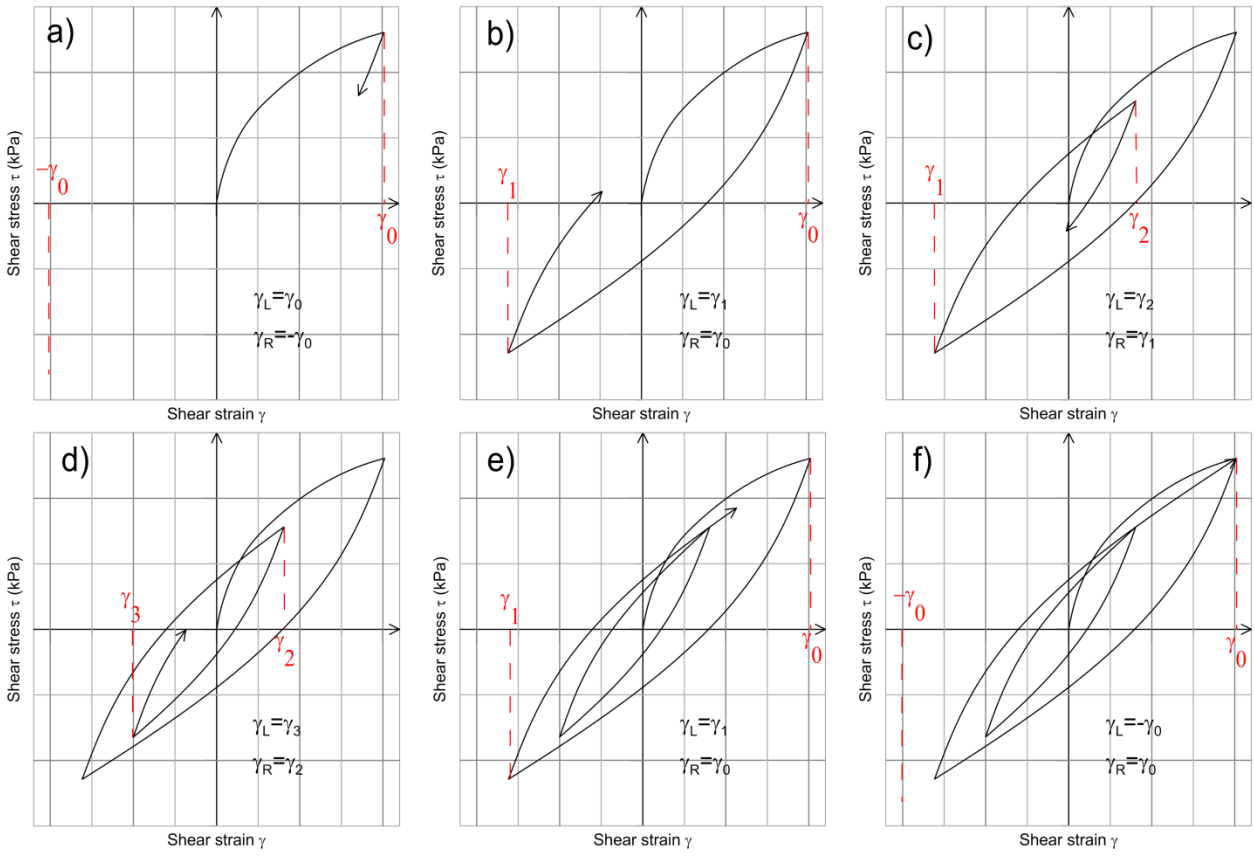

Figure 3.6 Evolution of the reversal strain vectors (Yniesta et al. (2017))

3.3 Viscous stress

In order to capture the strain rate dependence of the soil's behaviour, a viscous stress is added to the inviscid stress (Equation 3.1). The viscid stress formulation is directly strain-rate dependent and is described in this section. The general viscous response of the model is defined with the following formulation:

$$\tau_{visc} = F.load.c_{visc}.\sqrt[6]{|\dot{\gamma}|} \qquad \text{Equation 3.17}$$

where c_{visc} is the viscous coefficient, $\dot{\gamma}$ the strain rate, *load* is the sign of unloading-reloading direction (*load* = +1 in the $+\gamma$ direction, *load* = -1 in the $-\gamma$ direction) and F is a coefficient that allows to have a realistic stress-strain curve when the viscous stress is added to the inviscid stress. The formulation of this coefficient is different during initial loading ($F = F_{bb}$) and during unloading reloading ($F = F_{ur}$). Details are given in the next section.

The formulation of Equation 3.17 is used in order to be consistent with the study from Sheahan et al. (1996) who observed that the shear strength increases linearly with the logarithm of the strain rate, and the increase per logarithmic cycle varies between 5 % and 20 %. The present formulation allows to capture this strain-rate dependency of the shear strength and the viscous coefficient c_{visc} can be computed according to the desired increase of shear strength. The definition of c_{visc} as a function of the desired increase is detailed in the next chapter.

3.3.1 Viscous stress during initial loading

During initial loading, at small strains, τ_{visc} could increase quickly from zero to a value much greater than τ_{inv} if the coefficient F was set to 1. This could lead to a discrepancy between the viscid and the inviscid stresses, and an unrealistic stress strain-curve as presented in Figure 3.7, arising from the direct dependency of τ_{visc} on $\dot{\gamma}$. In order to obtain a more realistic stress-strain curve, the viscous stress is modified with a coefficient F (denoted F_{bb} during initial loading) so that it slowly increases with shear strain:

$$F_{bb} = \frac{1}{\sqrt{1 + (\frac{\delta_r}{\gamma})^d}} \qquad \text{Equation 3.18}$$

where γ is the shear strain, d is a constant equal to 4 and δ_r is a reference shear strain set equal to 0.015 %. The values of the parameters d and δ_r are independent of soil characteristics, and set so that the stress-strain curve is realistic. The coefficient F_{bb} is defined to obtain a progressive increase in viscous stress (Figure 3.7). Figure 3.8 describes the variation of the coefficient F_{bb} as a function of shear strain. At low shear strains, the value of the coefficient is low and so is the associated viscous stress. On the contrary, at higher strain values the coefficient is equal to 1 and the viscous stress recovers its maximum value.

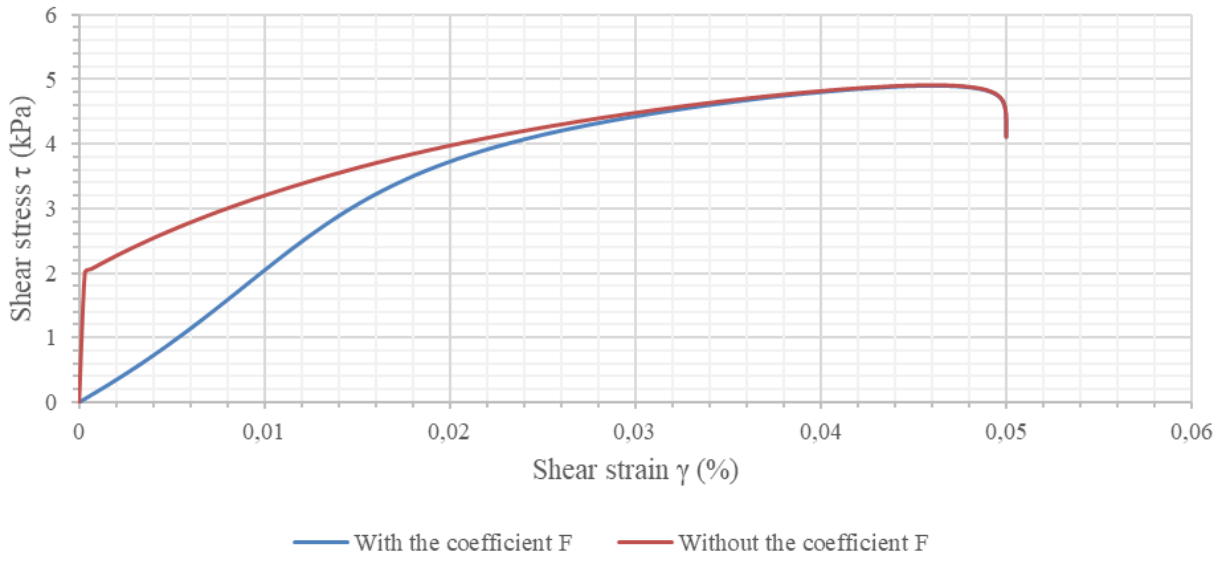

Figure 3.7 Comparison of the backbone curve with and without coefficient F_{bb}

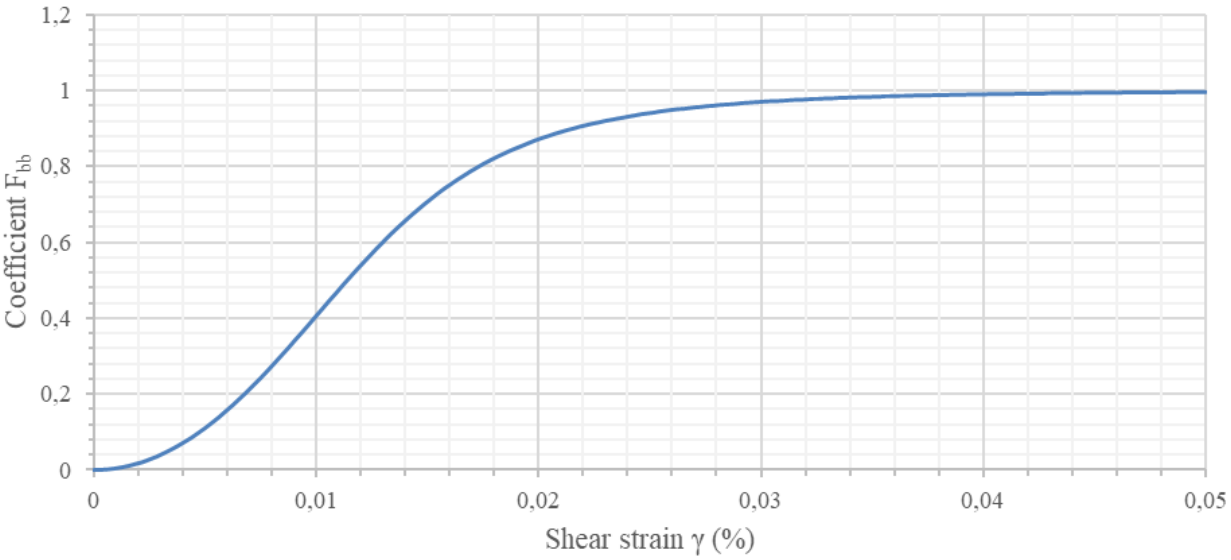

Figure 3.8 Coefficient F_{bb} during initial loading (backbone)

3.3.2 Unloading-reloading behaviour

During a change of direction, a gap in the stress strain curve would arise because of a change in signs of the direction of loading, if a coefficient F was not introduced (Figure 3.9). According to Equation 3.17, the sign of the viscous shear stress changes when a change of the loading direction is detected. To remove this gap, a coefficient F_{ur} is added to the formulation so that the viscous shear stress progressively goes from a positive (or negative) to a negative (or positive) value. The

formulation of F_{ur} is based on the target (F_R) and previous values of reversal coefficient (F_L) that the model keeps track of, at each reversal of loading, similarly to reversal stress-strain points.

When unloading happens after initial loading,the value of the coefficient F_{ur} at the reversal point is defined as the previous reversal coefficient $F_L = F_{bb}$, and the target reversal coefficient is defined as $F_R = -F_{bb}$. When a change of loading direction happens during unloading or reloading, F_L is set as the current value of F_{ur} and F_R takes the previous value of F_L. When a reloading cycle exceeds F_R, the current values of F_L and F_R are deleted, and the previous values of F_L and F_R are reinstated. At any shear strain, the coefficient is defined as follows:

$$F_{ur} = \frac{\left(2000^{\frac{1}{3}} + 0.5\right)\left(|F_L| + |F_R|\right)}{\left(\frac{4000 \cdot \gamma_c}{\gamma - \gamma_L}\right)^{\frac{1}{3}} + 0.5} - |F_L| \qquad \text{Equation 3.19}$$

The formulation of the coefficient has been chosen in order to satisfy the following conditions:

- upon a change of loading direction, the coefficient is equal to minusthe absolute valueof the previous reversal coefficient F_L;
- when the target strain is reached ($\gamma = \gamma_R$), the coefficient is equal to the absolute value of the target reversal coefficient F_R;
- during unloading-reloading, the observed gap should be removed and replaced by a realistic round tip. The values in the equation were set to obtain a reasonable shape of the stress-strain curve by trial and error, under different loading conditions.

We compare the stress-strain loops generated by the viscoplastic model during single element shear tests using a sinusoidal signal with an amplitude of 0.05 % and a loading frequency of 0.01 Hz with and without coefficient F (Figure 3.9). By comparing the stress-strain loops, the coefficient ensures a continuity at the reversal point and thus removes the gap at small strains and during a change of direction. Figure 3.10 represents the variation of the coefficient F_{ur} during the simulation, and illustrates how this coefficient evolves during two cycles of loading.

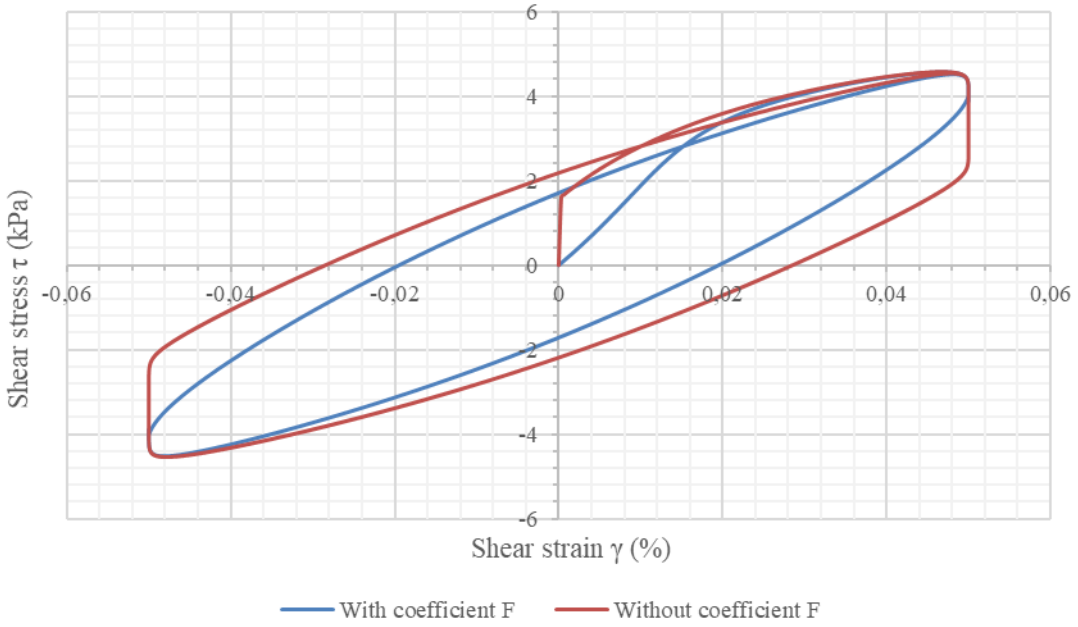

Figure 3.9 Comparison of the stress strain curve with and without *F*

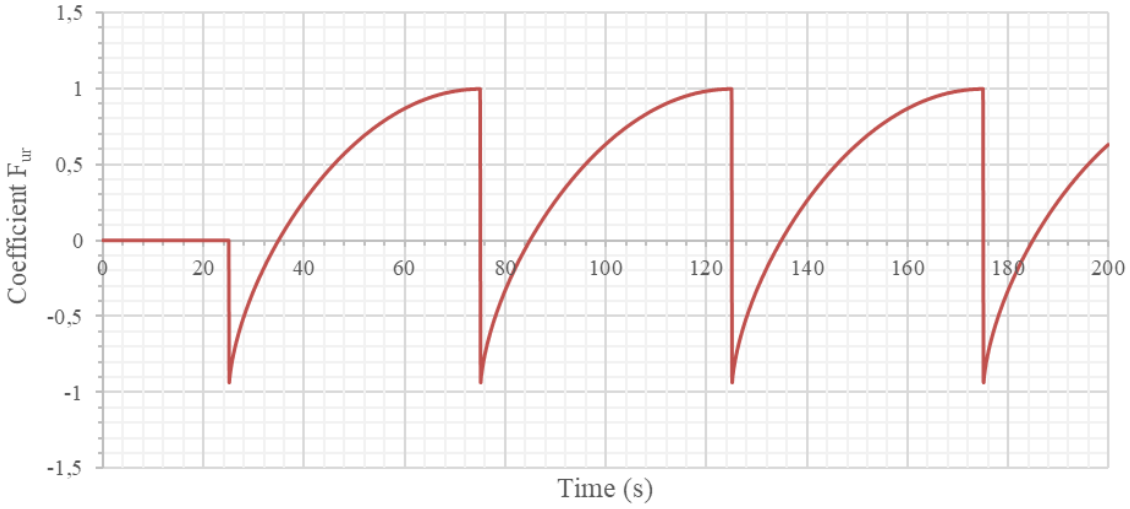

Figure 3.10 Coefficient F_{ur} during unloading-reloading

CHAPTER 4 TYPICAL PREDICTIONS OF THE MODEL

4.1 Introduction

The viscoplastic model was first implemented in a Mathcad routine to study its predictive capabilities in single element simulations. Once the model was validated, it was implemented in the ground response analysis software Deepsoil (Hashash et al. 2016). The implementation in Deepsoil and the use of the model in ground response analysis are presented in Chapter 5. The present chapter focuses on the validation of the constitutive equations presented in Chapter 3, and a description of the typical behaviour of the model. To do so, several simulations are presented in the sections below. The soil used for all the simulations was generically defined as a soft clay under the following conditions and with the following soil properties:

- Vertical effective stress σ'_v= 78.7kN/m^2
- Unit weight γ = 16.5 kN/m^3
- Overconsolidation ratio *OCR* =1
- Plasticity index *PI* = 12
- Shear wave velocity V_s = 100m/s

The maximum shear modulus G_{max} was calculated based on V_s using Equation 2.1, and the modulus reduction and damping curves were calculated from the empirical relationships introduced by Darendeli (2001) which depend on the previous properties. The modulus reduction curve is defined by Darendeli as a hyperbola as follows:

$$\frac{G}{G_{max}} = \frac{1}{1 + (\frac{\gamma}{\gamma_r})^{\alpha}} \qquad \text{Equation 4.1}$$

Where α and γ_r are parameters that depend on OCR, PI, and σ'_v. Based on the modulus reduction curve and Masing rules, Darendeli provides equations for the damping curve, too lengthy to be reproduced here. The obtained curves are shown in Figure 4.1.

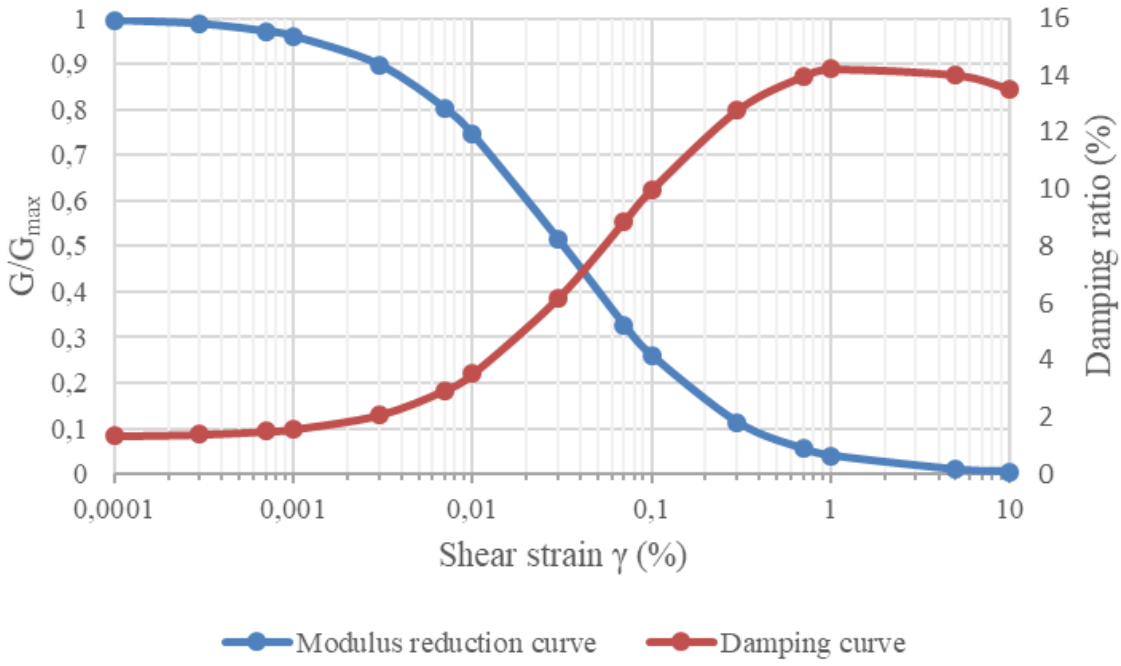

Figure 4.1 Input modulus reduction and damping curves

4.2 Strain rate dependency of shear strength

4.2.1 Definition of the viscous coefficient as a function of shear strength increase

Sheahan et al. (1996) observed that the shear strength increases linearly with the logarithm of the strain rate with an average increase between 5 % and 20 % per logarithmic cycle of strain rate. The equations of the viscoplastic model presented in Chapter 3 were specifically derived so that the response of the model would be consistent with those observations. The viscous stress introduced by the model is proportional to the viscous coefficient c_{visc} which can be calibrated based on a desired increase in shear strength per logarithm of shear strain rate (r_{su}). The definition of the viscous coefficient c_{visc} as a function of the increase of shear strength is demonstrated in this section.

Assume that a single element of soil is monotonically loaded at a strain rate of 10 %/s which remains constant during the simulation, up to a 10 % shear strain level, and that the shear strength is reached at this level of shear strain. The total stress, based on Equation 3.1, is described in Equation 4.2:

$$\tau(10\%) = \tau_{inv}(10\%) + \tau_{visc}(10\%)$$ Equation 4.2

$$\tau(10\%) = BB(10\%) + c_{visc}\sqrt[6]{10\%/s}$$ Equation 4.3

Where $BB(10\%)$ is the shear stress at 10 % taken from the input backbone curve, which is calculated from the input modulus reduction curve. This represents the shear strength obtained at a given strain rate assumed to be slow, which is equivalent to the monotonic undrained shear strength commonly measured in lab tests (S_u). We can divide the total stress τ by τ_1, corresponding to the total stress reached at 10 % with a strain rate of 10^{-2} %/s, which corresponds to the shear strength associated with a strain rate of 10^{-2} %/s.

$$\frac{\tau(10\%)}{\tau_1(10\%)} = \frac{BB(10\%)}{\tau_1(10\%)} + \frac{c_{visc}\sqrt[6]{10\%/s}}{\tau_1(10\%)}$$ Equation 4.4

The ratio $\frac{\tau(10\%)}{\tau_1(10\%)}$ depends on the desired increase r_{su} of shear strength per logarithmic cycles of strain rate, and since there are 3 logarithmic cycles between 10^{-2} %/s and 10 %/s, the previous equation can further be rewritten as follows:

$$(1 + r_{su})^3 = \frac{BB(10\%) + c_{visc}\sqrt[6]{10\%/s}}{BB(10\%) + c_{visc}\sqrt[6]{10^{-2}\%/s}}$$ Equation 4.5

Rearranging the previous equation yields:

$$c_{visc}\left(\sqrt[6]{10\%/s} - (1 + r_{su})^3\sqrt[6]{10^{-2}\%/s}\right) = BB(10\%)((1 + r_{su})^3 - 1)$$ Equation 4.6

The equation obtained allows to calculate c_{visc} as a function of the desire increase r_{su} and also the inviscid stress at 10 % strain i.e. the monotonic shear strength associated with the input modulus reduction curve:

$$c_{visc} = \frac{BB(10\%)((1 + r_{su})^3 - 1)}{\left(\sqrt[6]{10\%/s} - (1 + r_{su})^3\sqrt[6]{10^{-2}\%/s}\right)}$$ Equation 4.7

4.2.2 Strain rate effects on the predicted shear strength

A single element of soil is monotonically loaded with different strain rates which remain constant during the simulation. Strain rates varied from 10^{-2} %/s to 10 %/s to be consistent with strain-rates observed during earthquakes (Sheahan et al. (1996), Lefebvre and LeBoeuf (1987)).

We compare the backbone curves obtained with the viscoplastic model at each strain rate (Figure 4.2) for different values of the viscous coefficient c_{visc} (Table 4.1) corresponding to different increase of shear strength per logarithmic cycles of strain rate (r_{su} in Equation 4.6). The inviscid backbone stress at 10 % strainis calculated based on the input modulus reduction curve. As expected, the shear stress increases with the increase of strain-rate and the higher the r_{su} coefficient, the larger the difference of shear stress gets between different strain-rates. Overall a higher r_{su} coefficient is associated with a stiffer response.

Table 4.1Viscous coefficient values depending on the shear strength increase

Shear strength increase per logarithmic cycle r_{su}	**Viscous coefficient c_{visc}**
5%	3.095
10%	7.114
15%	12.489
20%	19.977

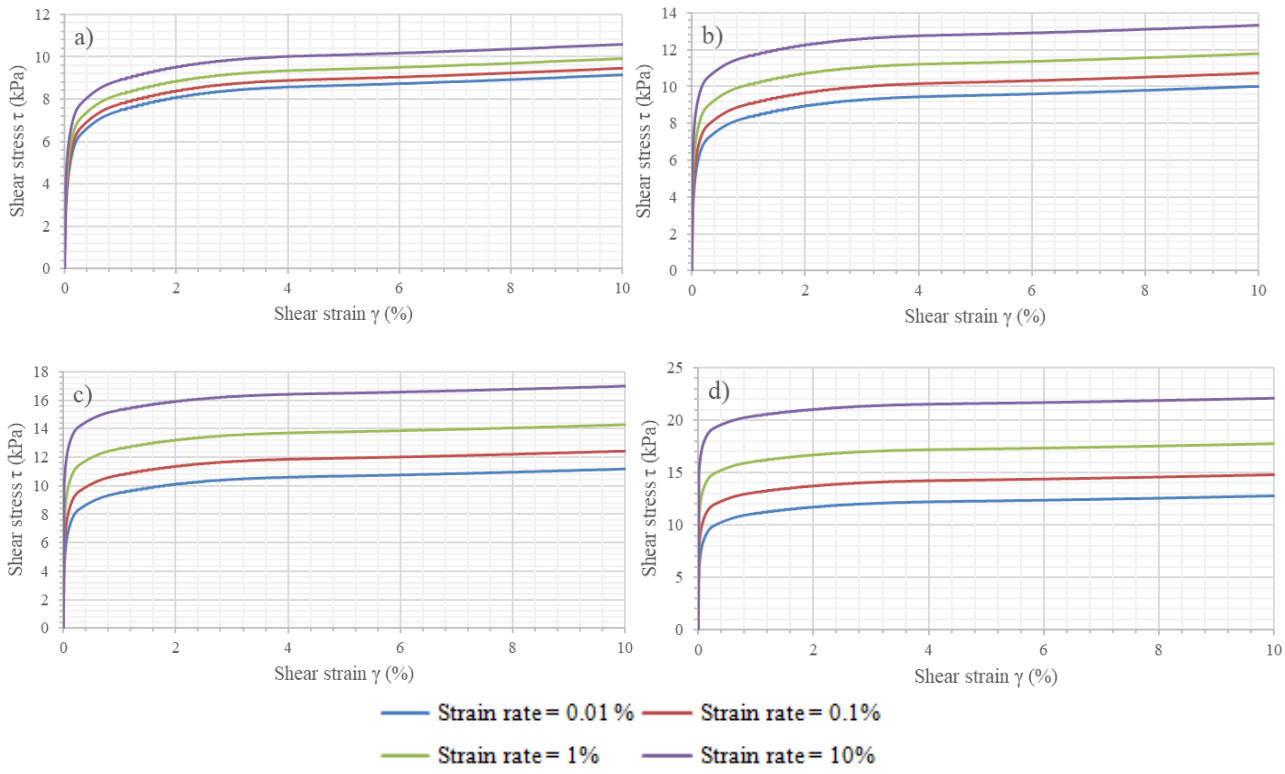

Figure 4.2 Backbone curve comparison with a) r_{su} = 5 %, b) r_{su} = 10 %, c) r_{su} = 15 %, d) r_{su} = 20 %

We plot the shear strength computed for each strain rate, taken as the shear stress at a 10 % strain level, normalized by the shear strength at a strain rate of 10^{-1} %/s, and we compare our results with Sheahan's observations. The viscoplastic model is able to capture reasonably the strain-rate linear dependency of the shear strength with the logarithm of the strain rateobserved by Sheahan et al (1996) in laboratory tests on clays (Figure 4.3), for a realistic range of shear strength increase (r_{su}), over a range of shear strain rate that correspond to what is observed during earthquakes. The curves from the model are not perfectly linear which allows for a more realistic behaviour, since a linear curve would indicate a shear strength close to zero for very low values of strain rate.

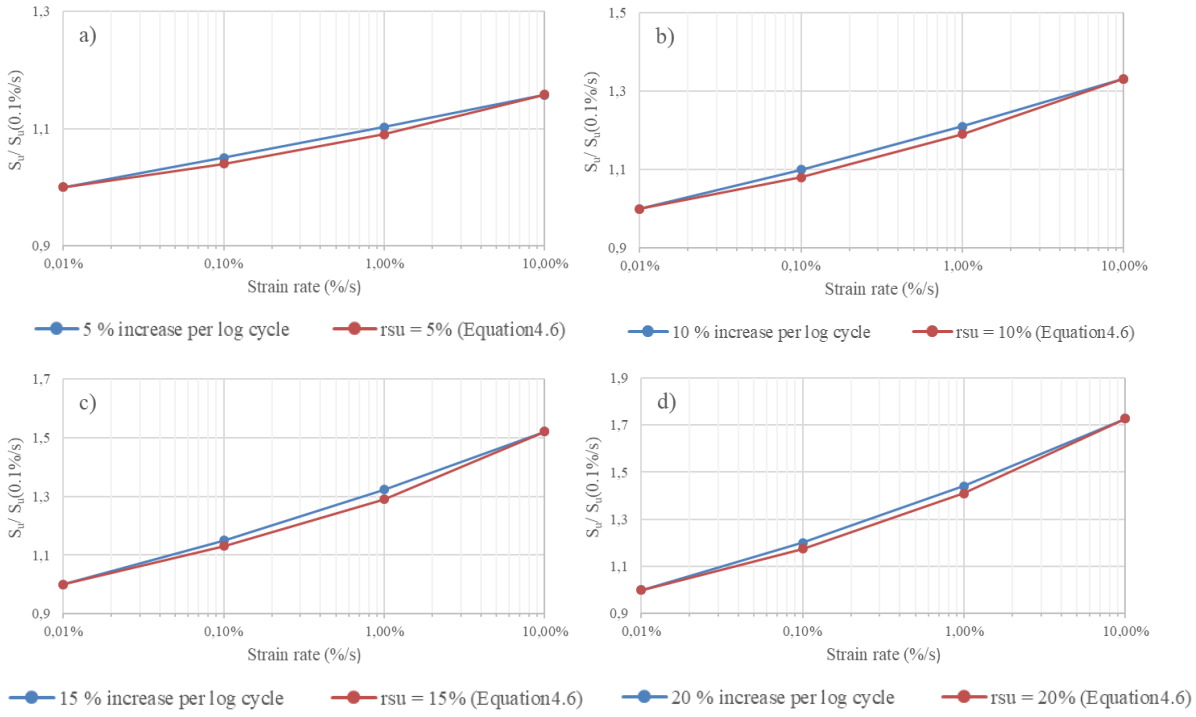

Figure 4.3 Shear strength increase per logarithmic cycle of strain rate a) r_{su} = 5 %, b) r_{su} = 10 %, c) r_{su} = 15 %, d) r_{su} = 20 %

4.3 Effect of viscous coefficient

The viscous behaviour of soils is integrated in the constitutive model by using the viscous coefficient c_{visc}. In this section, the effect of the viscous coefficient on the stress-strain curve and on the damping curve is presented through different examples of single element simulations.

4.3.1 Effect of viscous coefficient on the stress-strain curve

In the simulation, the soil was cyclically loaded with a sinusoidal function with a constant amplitude of 1 % and a loading frequency of 0.01 Hz (Figure 4.4).

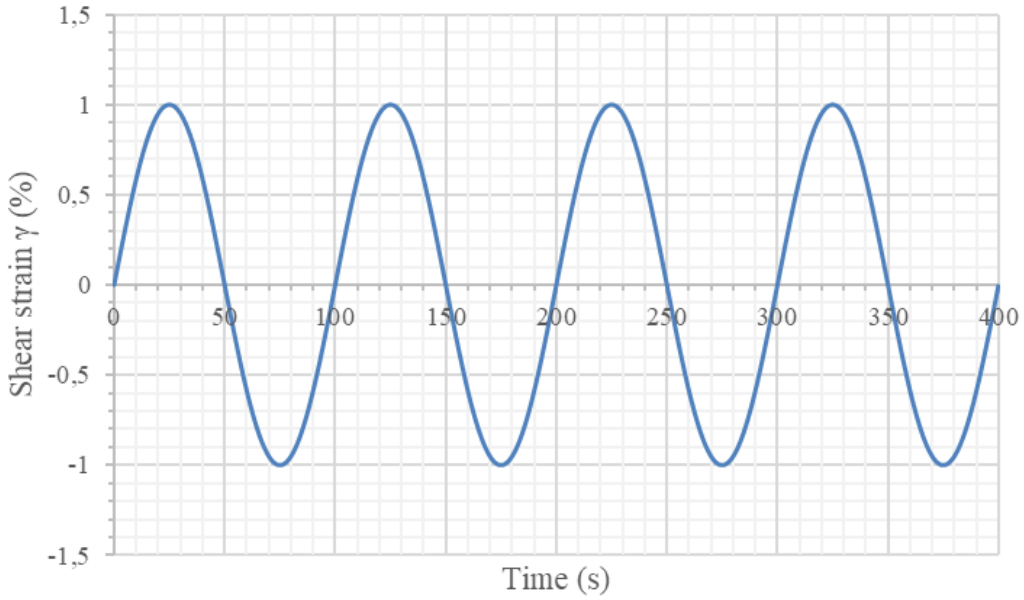

Figure 4.4 Input strain

Simulations were performed with different values of viscous coefficient c_{visc} corresponding to different increase of shear strength with the logarithmic cycle of strain rate based on Equation 4.6. Figure 4.5 presents the results of the simulations using the viscoplastic model. The overall stiffness of the model increases with c_{visc}, because the viscous stress τ_{visc} increases somewhat linearly with the viscous coefficient, and the backbone curve exhibits a stiffer behaviour due to the added viscous stress. When c_{visc} is equal to zero, the model is equivalent to the plastic model presented in Yniesta et al. (2017). During unloading-reloading, the c_{visc} induces a higher hysteretic damping, as illustrated by the shape of the loops. The next section studies in depth the effect of the viscous coefficient on the damping behaviour.

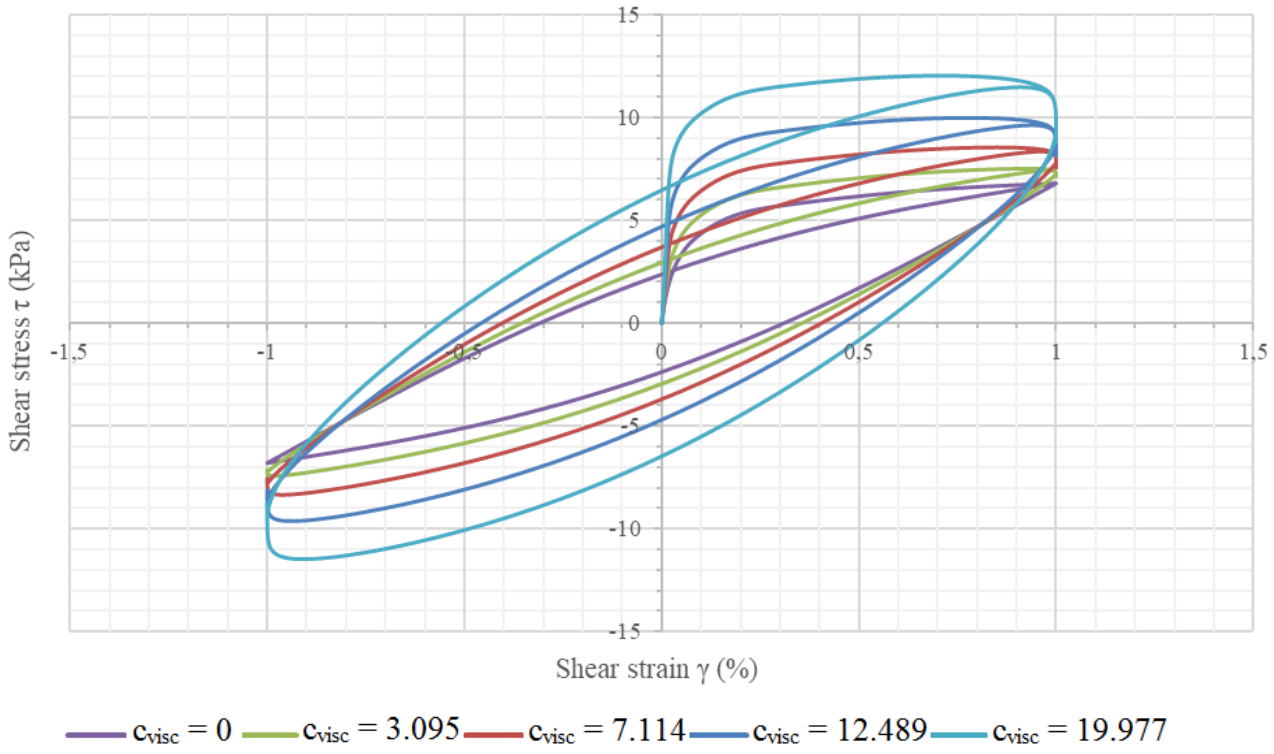

Figure 4.5 Effect of c_{visc} coefficient on the stress-strain curve

4.3.2 Effect of viscous coefficient on damping curve

4.3.2.1 Damping calculations

Damping is an essential parameter for describing the cyclic behaviour of soil. It represents the capacity of a soil to dissipate energy within a vibrating or a cyclically loaded system. In Figure 3.4, the energy dissipated over a loading cycle isrepresented by the red area in the hysteresis loop (*2A*). The hysteretic damping ratio is calculated based on Equation 3.11 repeated here for convenience:

$$D = \frac{2A}{4\pi B}$$

Where A is the area of the half loop and B is the area of the triangle representing the work developed if the soil behaved linearly.

4.3.2.2 Damping curve for different viscous coefficients

The model from Yniesta et al. (2017) reproduces any input damping curve by using a coordinate system transformation. The presented model includes a strain-rate dependency which will inevitably introduce a discrepancy between the target and obtained curve. This example studies the difference between the target damping curve and the damping obtained from the viscoplastic model in a single element shear test simulation. The element of soil is cyclically loaded with a sinusoidal function withamplitudes ranging from 10^{-4} % to 10 % (Figure 4.6) and a loading frequency of 0.1 Hz.

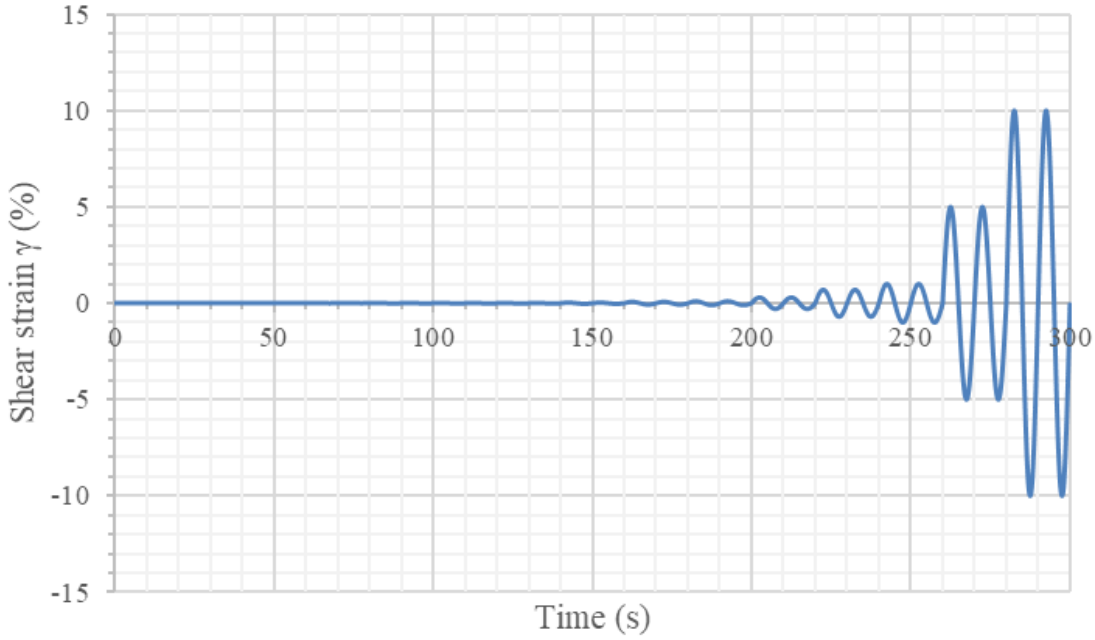

Figure 4.6Input sinusoidal function with increasing shear strain amplitude

For each shear strain amplitude, the damping is calculated based on Equation 3.11 for both the viscoplastic and the plastic model. For the viscoplastic model, a viscous coefficient corresponding to an increase of 5 %, 10 %, 15 % and 20 % of shear strength with the logarithmic cycle of strain rate is used.

The damping curve obtained with the plastic model (Yniesta et al. (2017)) and the new viscoplastic model, with different values of the viscous coefficient (Table 4.1), are presented in Figure 4.7. The viscous coefficient induces a higher hysteretic damping, as illustrated by the shape of the curve. The damping increases with the viscous coefficient, but is unaffected at small

strains. Although the increase in damping is not controlled, the results obtained remain acceptable, and consistent with Darendeli's observations (2001) as detailed in the next section.

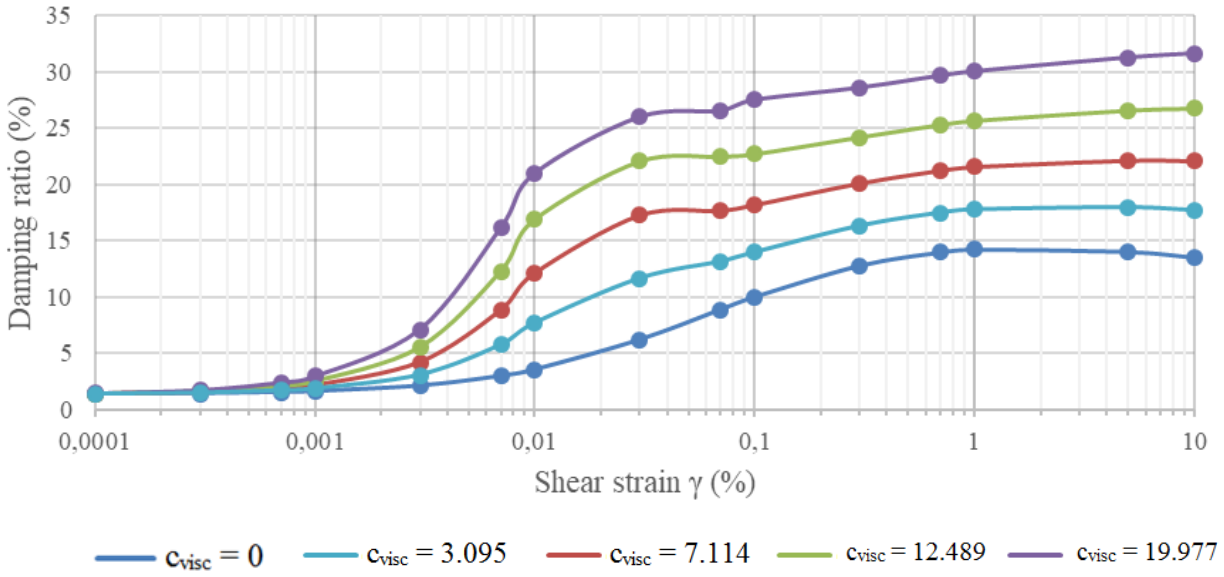

Figure 4.7 Effect of c_{visc} coefficient on damping curve

4.4 Effects of strain rate and frequency on damping behaviour

In order to assess the effects of strain rate and frequency on the damping behaviour of the model, we perform cyclic shear tests simulations on a single element at different loading frequencies and strain rates, and study the damping response of the model.

4.4.1 Frequency effects on damping behaviour

In the simulations the viscous coefficient is set to correspond to an increase of 10 % of shear strength, and the element of soil is cyclically loaded with a sinusoidal function with amplitudes ranging from 10^{-4} % to 10 % and loading frequencies of 0.01 Hz, 0.1 Hz and 1 Hz. Damping is then calculated at every frequency and at every amplitude by computing the area under the curve and using Equation 3.11.

Figure 4.8 presents a comparison of the damping using different frequencies. The viscous stress induces a higher hysteretic damping, as illustrated by the shape of the curve, which is consistent with Darendeli's observations (Darendeli 2001) stating that damping increases with loading frequency. At very low strain (0.0001 to 0.001%), damping stays constant for the different

frequencies, which is consistent with the study of Vucetic et al. (1998) who indicated that at very small strain levels material damping in soils is frequency independent.

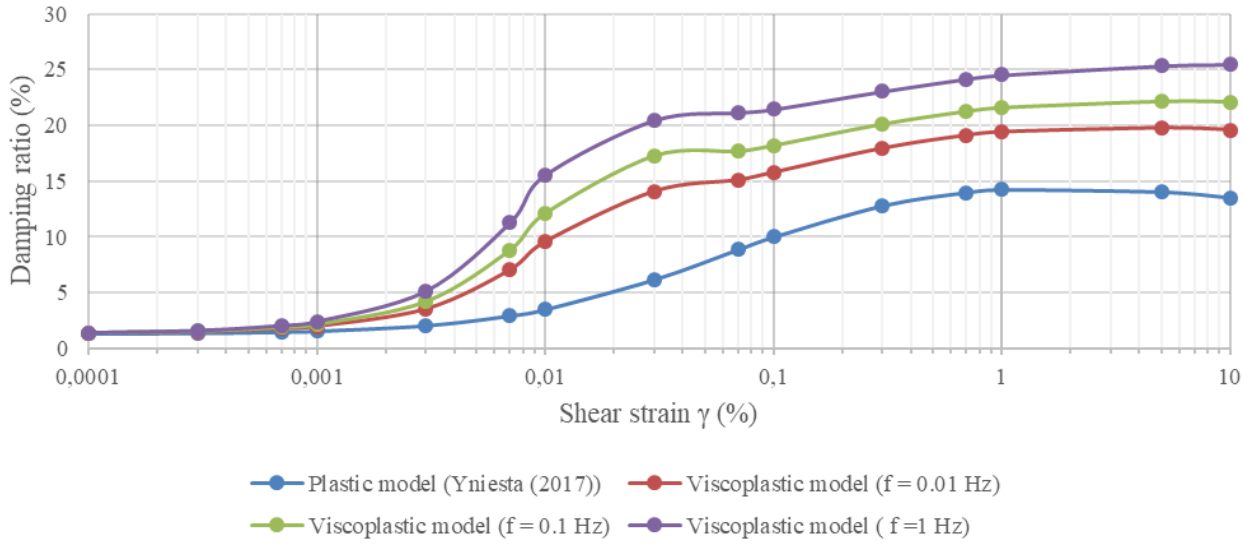

Figure 4.8 Effect of frequency on damping curve

4.4.2 Strain rate effects on damping behaviour

The element of soil is cyclically loaded with a triangular function with amplitudes ranging from 10^{-4} % to 10 % and strain rates of 10 %/s, 1 %/s and 0.1 %/s. Damping is then calculated for each strain rate at every amplitude. Figure 4.9 presents a comparison of the damping. As expected, the increase of strain rate induces a higher hysteretic damping, as illustrated by the shape of the curve, which is similar to what is being observed for different loading frequencies.

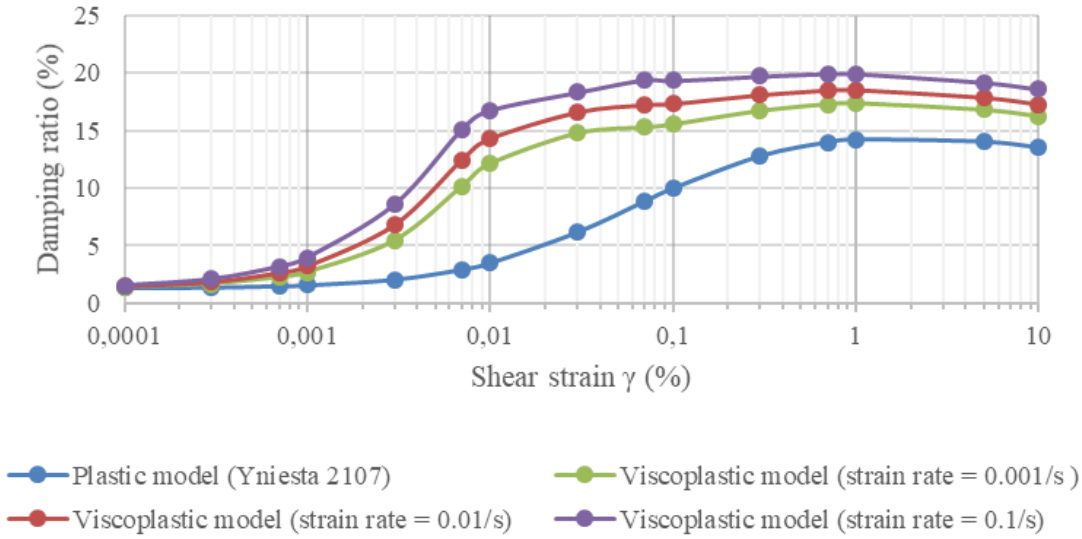

Figure 4.9 Effect of strain-rate on damping curve

4.5 Examples of typical simulations

4.5.1 Comparison of triangular and sinusoidal signal

4.5.1.1 Input parameters

In order to further study the strain rate dependency of the viscoplastic model, we compare the stress-strain loops generated by the model using a viscous coefficient equal to 7.114 (r_{su} = 10%), during single element shear tests done with a sinusoidal and a triangular signal (Figure 4.10). The behaviour of a soil under each type of signal should differ because of strain-rate effects, since in a triangular signal the strain rate is constant whereas the strain rate of the sinusoidal signal varies.It has been observed that soils often exhibit rounded tip upon sinusoidal loading which increases the energy dissipated during cyclic loading (i.e. the damping response of the soil) (Vucetic et al. 1998). The two signals have the same cyclic amplitude of 1 % with a loading frequency of 0.1 Hz.

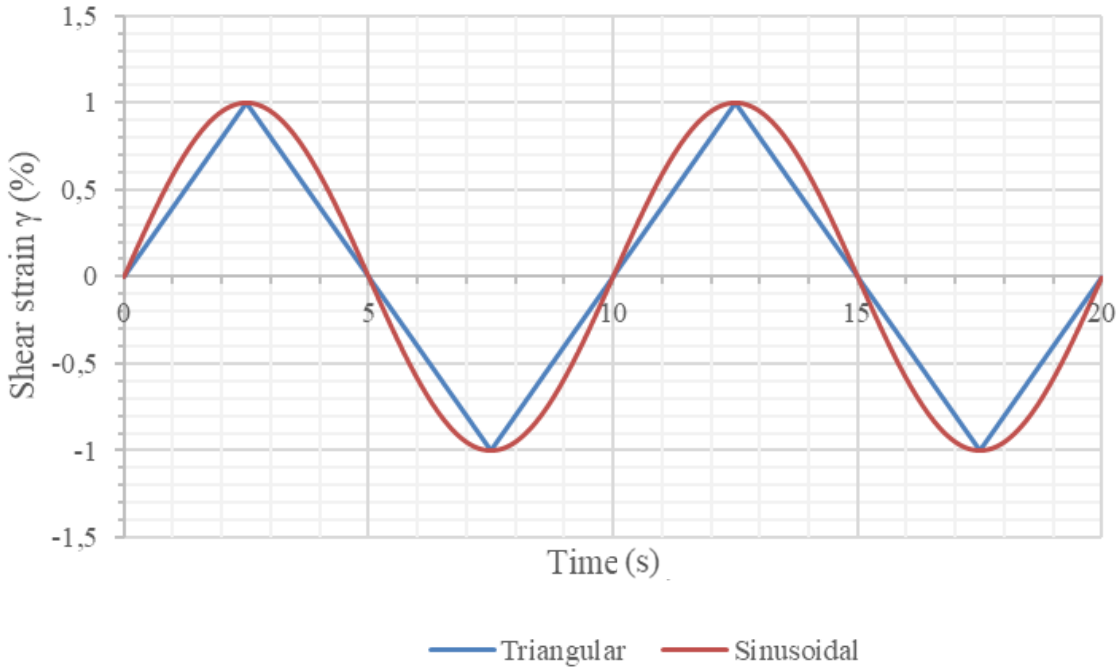

Figure 4.10 Input signals

4.5.1.2 Stress-strain comparison

The simulations using the ARCS model yield identical response for both signals since the model does not include strain-rate dependence (Figure 4.11), while the response of the viscoplastic model is stiffer during initial loading when subjected to sinusoidal signal, because the initial strain rate is higher.

At the peak of the sinusoidal signal, the strain rate decreases and the shear stress decreases as well, while the strain-rate of the triangular signal is still constant. The hysteretic loops obtained with a sinusoidal loading are slightly larger, indicating a slightly higher damping, which is consistent with the observed behaviour of soils (Vucetic et al. 1998).

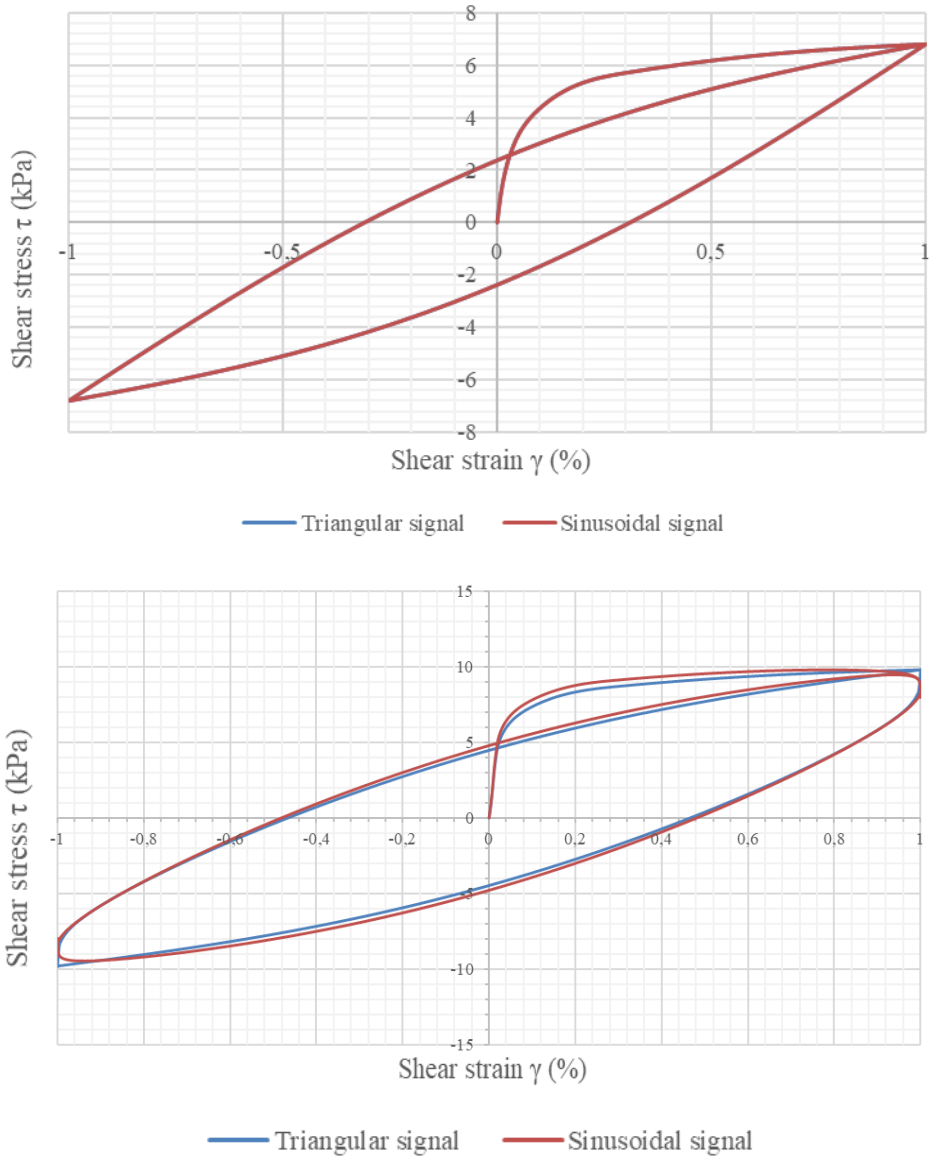

Figure 4.11 Stress-strain curve comparison using a) ARCS model b) Viscoplastic model

4.5.2 Earthquake broadband signal

This section presents an example using the viscoplastic model with an earthquake as input signal and a viscous coefficient corresponding to 10 % increase of shear strength. The results are compared with those obtained with the ARCS model.

4.5.2.1 Input motion

A realistic soil profile was simulated in a ground response analysis simulation using the software Deepsoil. The input motion was a recording from the Northridge earthquake (M_w = 6.7) recorded

at the Long Beach City Hall, with a maximum acceleration of 0.098g. Strain time series were retrieved at a depth of 12 m, corresponding to an effective stress of 78.7 kN/m^2, and used as an input parameter in Mathcad (Figure 4.12).

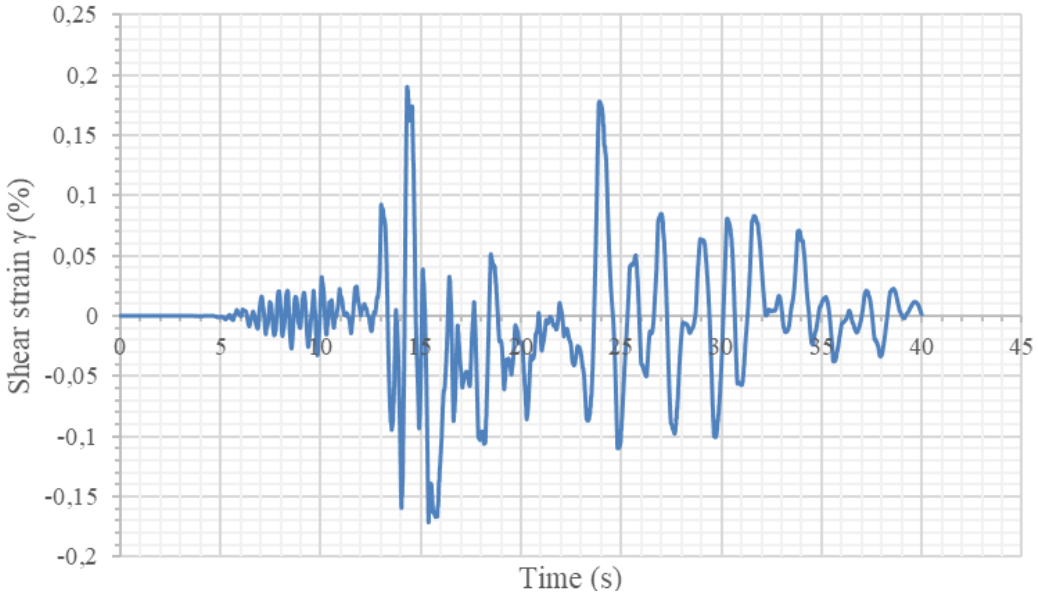

Figure 4.12 Input strain time series

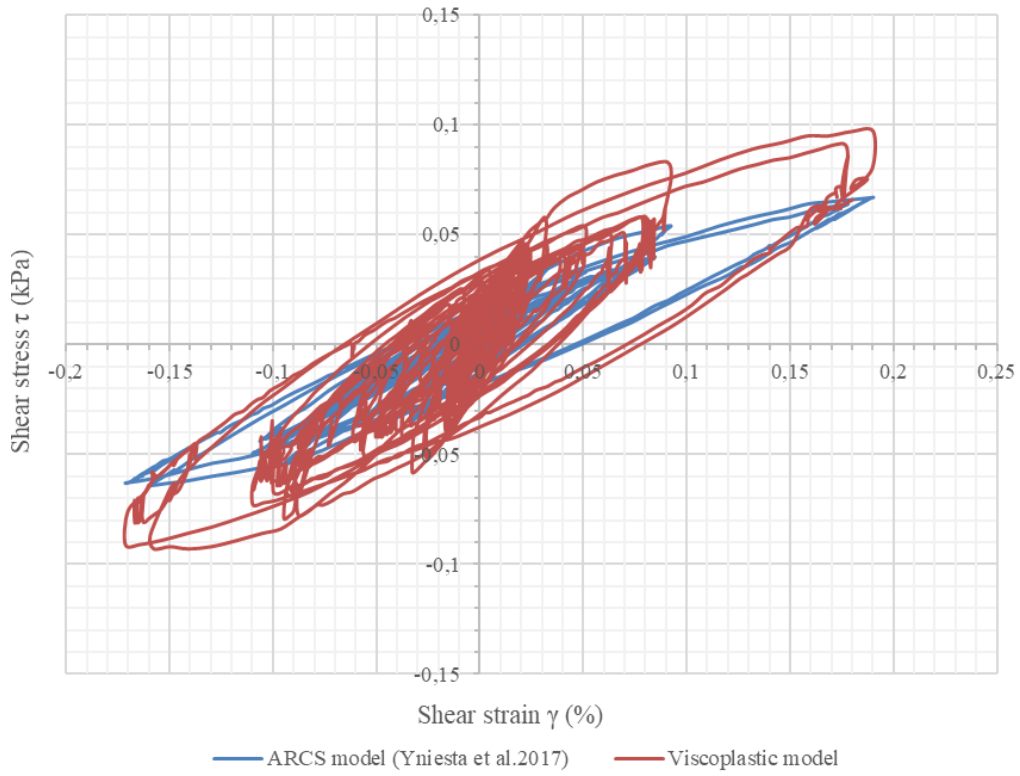

Figure 4.13 Stress-strain curve

The viscoplastic model provides a different prediction of the stress-strain curve compared to the plastic model (Figure 4.13). This difference is due to the added viscous stress that depends on the strain-rate. During the simulation, strain-rate varies and results in a change in the stress–strain curve by inducing a higher hysteretic damping as discussed in the section 4.3.2. The shape of the stress-strain curve using the viscoplastic model has rounded points at the unloading-reloading points close to the results obtained with sinusoidal loading (section 4.5.1) which is consistent with Vucetic et al (1998) observations.

4.6 Limitations of the model

Although the model is able to reproduce the effects of loading frequency and strain rate on the damping behaviour (Figure 4.8 and Figure 4.9) the damping response is not quantitatively controlled, which is a major limitation of the viscoplastic model. During an earthquake, sudden changes of shear strain lead to large strain-rates and thus large viscous stresses which can result in a sudden change in the shape on the stress-strain curve.

On the other hand, the proposed viscoplastic model can control the increase of shear strength depending on strain-rate based on Sheahan's observations (section 4.2), for any increase included in 5 % and 20 %, which is an important feature of the soil's response. However, the increase in shear strength is mostly related to an overall increase in stiffness (Isenhower and Stokoe 1981), and the model would not be able to include this effect, since the strain rate dependency of the model's behaviour is stronger at large strains than low strains.

CHAPTER 5 DEEPSOIL IMPLEMENTATION AND COMPARISON WITH CENTRIFUGE MODEL

The viscoplastic model introduced earlier is implemented in the one-dimensional site response analys is program Deepsoil. This section introduces the software and explains how the viscoplastic model was implemented. In order to study the performance of the model, a suite of centrifuge tests (Afacan et al. 2014) is simulated and the results of ground response analyses are compared with the measurements. This comparison is detailed in section 5.3.

5.1 Introduction to Deepsoil

Deepsoil is a one-dimensional ground response analysis program that can perform linear, equivalent linear and nonlinear analysis. The software has first been developed by Youssef M.A. Hashash and Duhee Park (Hashash and Park 2001), and modified subsequently under the leadership of the former, leading to the most recent version (Hashash et al. 2016). For the nonlinear analysis, the soil is represented by a lumped mass model, where each layer is represented by a mass, a nonlinear spring and a dashpot where the equation of motion (Equation 2.2) is solved in time domain using the Newmark β method (1959). In Deepsoil, a variety of nonlinear models is available for the analyses during initial loading and unloading-reloading.

5.1.1 Backbone curve

The backbone curve can be calculated based on the following models:

- MKZ model: It was developed by Matasovic (1993) and based on the hyperbolic model by Konder and Zelasko (1963). It is a pressure-dependent hyperbolic model that improves the ability to capture small-strain behaviour. It may overestimate or underestimate the maximum shear stress
- GQ/H model: It was developed by Groholski et al. (2016) and is the latest model implemented in Deepsoil. This model can control the shear strength and can match a modulus reduction curve

5.1.2 Unload-reload curve

- MR, MRD, DC models: These are different procedures to approach the Masing rules. As mentioned in Chapter 2, the use of Masing rules in site response analysis programs is associated with an inherent misfit of the damping curve. Nonlinear codes have dealt with this issue by adjusting the modulus reduction curve. For instance, MR, MRD and DC models allows to find parameters that give the best fit for either the modulus reduction or the damping curve with potentially a misfit of one of them.
- MRDF model: the MRDF Pressure-Dependent Hyperbolic (Phillips and Hashash 2009) model is the most advanced non-Masing unload-reload rules. Phillips and Hashash (2009) modified the Masing unloading-reloading rules by using a reduction factor in order to provide a better fit of the damping curve at large strains.

5.2 Implementation of the model in Deepsoil

In order to implement the viscoplastic model in Deepsoil, the model was coded in C++ and compiled using Visual Studio as a dynamic link library (DLL). The DLL is then loaded in Deepsoil so that the viscoplastic model can be used as an integrated model into the software.This section summarizes the implementation and explains the fundamental algorithm of the model.

5.2.1 Input parameters

Input parameters are divided into standard and model-specific inputs. The standard input parameters represent the parameters needed by Deepsoil for every layer regardless of the constitutive model. Standard inputs are:

- layer index, since every layer is numerated from 1 to the number of layers;
- maximum shear modulus G_{max}, computed from the input shear wave velocity;
- unit weight;
- thickness of the layer;
- minimum damping ratio D_{min};

The model-specific inputs are necessary parameters for the viscoplastic model. For every layer, the following parameters need to be defined.

- Input strain vector, which describes the 15 cyclic shear strain levels at which the two input curves (see below) will be defined. The number of input points was chosen based on what engineers typically consider in practice to define MRD curves.
- Modulus reduction curve, defined with a vector of 15 modulus reduction values associated with the strain level contained in the input strain vector.
- Damping ratio curve, which defines the damping ratios at all 15 strain levels as well.
- Viscous coefficient r_{su} representing the desired increase of shear strength per logarithm cycle of strain rate.

5.2.2 State variables

The algorithm uses a range of state variables that are updated at every time step. For all constitutive models, there are at least two state variables, the shear strain and the shear stress. At every time step, the model is provided a new shear strain and the goal is to update all the state variables and return the new shear stress. Besides stress and strain, the state variables included in the modelare the vectors of target and previous reversal stress-strain points (γ_L,τ_L,γ_R,τ_R), defined as stacks. The coefficient F_R and F_L used to compute the viscous strain part of the models and described in section 3.3 are also being tracked by using stacks, following a similar logic.

5.2.3 Initialization

The initialization process allows to read the input parameters and assign them to variables. Modulus reduction and damping vectors are associated to the previous input strain and the modulus reduction curve is then translated to a backbone curve using the maximum shear modulus G_{max}. The coefficients of the cubic spline fit of the backbone curve are then calculated and the viscous coefficient c_{visc} is calculated based on the increase r_{su} per logarithm of shear strain (Equation 4.7).

5.2.4 Constitutive model function

The main function of the viscoplastic model takes a new strain calculated by Deepsoil and returns a new stress based on the constitutive equations of the viscoplastic model. At the beginning of the time step the algorithm computes the strain increment and set the values of the variables that need to be updated at every time step, to the value of the previous time step. The model then separates response in initial loading and the unloading-reloading part, based on whether the current shear strain is greater than the maximum shear strain ever reached.

5.2.4.1 Backbone curve

When the current shear strain is greater than the maximum shear strain, the model is considered in initial loading, current stacks are emptied, and the current shear strain becomes the maximum shear strain. The total stress is calculated by summing the inviscid stress calculated with the cubic spline interpolation and the viscous stress calculated based on Equation 3.17.

5.2.4.2 Unloading-reloading curve

If the current shear strain is not greater than the maximum strain, the model is either unloading or reloading. To define the unload-reload curve, the previous and target reversal parameters are first determined before computing the new stress.

5.2.4.2.1 Update of target and previous stress-strain points

If a change of direction is detected by a change of sign of the strain increment, the values of previous and target reversal stress-strain points are updated. After the initial loading, the previous and target reversal stress-strain points are defined respectively as the inviscid unloading point and the symmetrical point of the latter. The value of the coefficient F_{ur} at the reversal point is defined asthepreviously reversal coefficient $F_L = F_{bb}$, and the target reversal coefficient is defined as $F_R = - F_{bb}$.

If the change of loading direction is detected from an existing unload-reload loop,the reversal point is defined as the previous reversal point, and the previous reversal point becomes the target reversal point. The coefficient F_L is defined as the current value of F_{ur} and F_R takes the previous value of F_L.

During unloading-reloading, when a reloading cycle exceeds the target strain point, the current values of the target and previous strain points are deleted, and the previous values of the target and previous strain points are reinstated. The coefficient F is updated following a similar logic, when a reloading cycle exceeds F_R, the current values of $F_L$andF_R are deleted and the previous values of F_L and F_R are reinstated.

5.2.4.2.2 Stress computation

If a change in previous or target reversal stress-strain point is detected, the coefficients of the biquadratic equation (Equation 3.13, Equation 3.14 and Equation 3.15) are recalculated. Once the coefficients are determined, the inviscid and viscous stress formulations described in Chapter 3 are used to compute the new stress. At each time step, function updates strain and returns a new stress.

5.3 Performance of the model in nonlinear ground response analysis

To study the performance of the viscoplastic model in nonlinear ground response analysis, a suite of centrifuge tests (Afacan et al. 2014) is simulated, and the results of the analysis are compared with the centrifuge tests data.

5.3.1 Introduction to centrifuge tests

Centrifuge tests are used in geotechnical engineering to model on a small scale specimen (the model) the behaviour of a large-scale system (the prototype). When centrifugal acceleration increases, the weight of the model increases, which permits to accurately simulate the behaviour of soils by having identical stresses in both model and prototype using a scale factor N corresponding to the level of centrifugal acceleration, since the soil behaviour depends on the confining pressure. The factor N allows to convert properties between the model and the prototype scale according to scaling laws. For instance, the ratio L^* defining the ratio of length measured in the model and length in the prototype is formulated by Equation 5.1:

$$L^* = \frac{1}{N} = N^{-1} \qquad \text{Equation 5.1}$$

Table 5.1 summarizes the centrifuge scaling laws for several parameters.

Table 5.1Scaling factors for centrifuge tests (Bruce L. Kutter 1992)

Quantity	Symbol	Units	Scale factor
Length	L	L	N^{-1}
Volume	v	L^3	N^{-3}
Mass	M	M	N^{-3}
Gravity	g	LT^{-2}	N
Force	F	MLT^{-2}	N^{-2}
Stress	σ	$ML^{-1}T^{-2}$	1
Module	E	$ML^{-1}T^{-2}$	1
Strength	s	$ML^{-1}T^{-2}$	1
Acceleration	a	LT^{-2}	N
Time (dynamic)	t_{dyn}	T	N^{-1}
Frequency	f	T^{-1}	N
Time (diffusion)	t_{dif}	T	N^{-1} or N^{-2}

5.3.2 Centrifuge models

Centrifuge tests were performed at the UC Davis center for geotechnical modeling on soft clay deposits interbedded with thin sandy layers, in order to study the nonlinear site response behaviour (Afacan et al. 2014a). The profile used during the tests consisted of an overconsolidated (OCR = 2.1 to 3.6) San Francisco bay mud underlying a lightly overconsolidated (OCR = 1 to 1.2) bay mud, and a layer of sand on top (Figure 5.1).

Table 5.2 summarizes the main properties of the bay mud and the sand used in the centrifuge model. The soil was placed in a hinged-plate container which consists of steel annular rings that are on ball bearings, rigid sidewalls and plates that can rotate (Figure 5.2). The container is flexible and its shear stiffness is practically zero thus avoiding wave reflections at the boundaries of the model. The model was heavily instrumented with accelerometers (ACC's), pore pressure transducers (PPT's), and linear potentiometers (LPT's) to measure the response of the model to imposed ground motions.

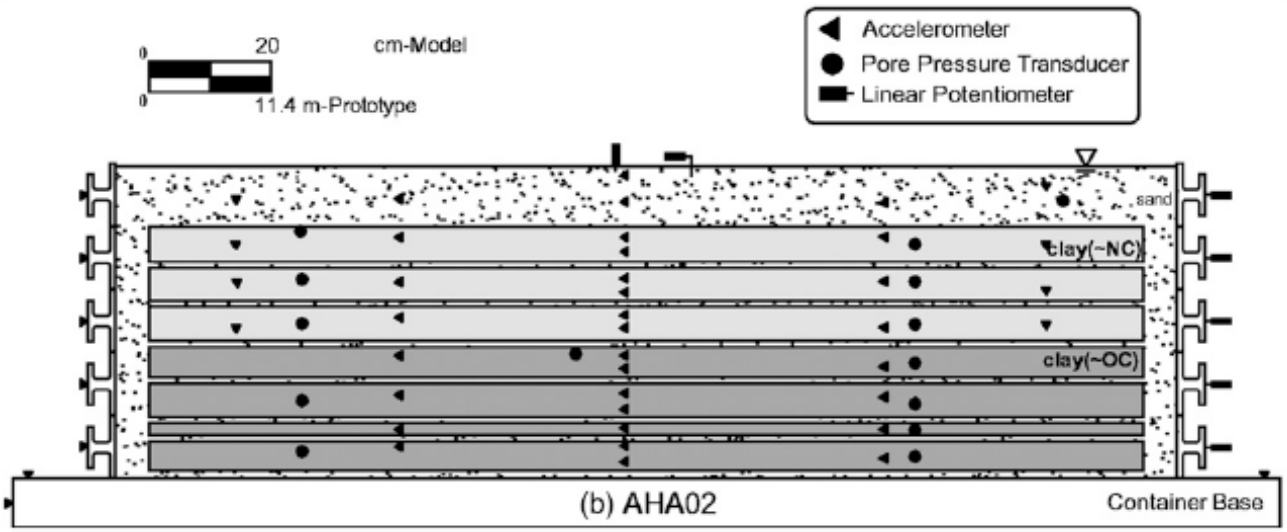

Figure 5.1 Profile of centrifuge model AHA02 (Afacan et al. 2014a)

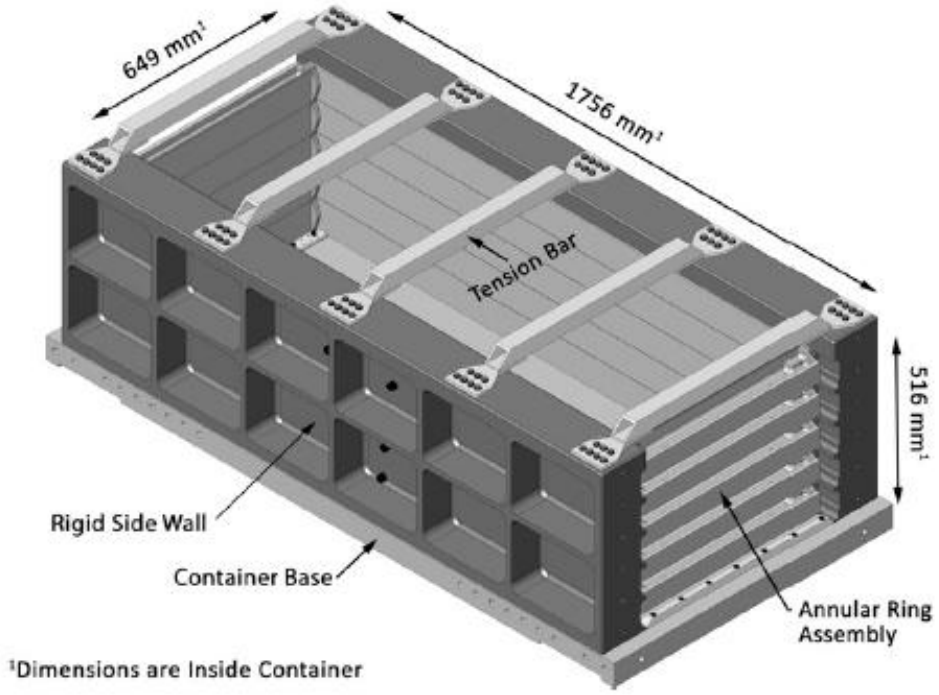

Figure 5.2 Container used in the centrifuge tests (Afacan et al. 2014a)

Table5.2 Soil properties used in the centrifuge tests(Afacan et al. 2014a)

Properties	**Bay mud**	**Sand**
Specific Gravity	2.65	2.64
Mean grain size, D_{50} *(mm)*		0.17
Coefficient of uniformityC_u		1.64
Relative density (%)		80
Unit weightγ(kN/m^3)	16-17	19.8
Compression index C_c	0.43	
Recompression index C_r	0.04	
Plasticity index *PI(%)*	40	
Liquid Limit *LL(%)*	84-86	
FC(%)	100	

Figure 5.3 presents profiles of vertical effective stress and preconsolidation pressure, shear wave velocity and undrained shear strengthof the studied profile. Shear wave velocity V_s was calculated based on the maximum shear modulus G_{max} which was deduced based on the following empirical relationship (Afacan et al. 2014a):

$$\frac{G_{max}}{p_a} = \alpha.\left(\frac{1+2K_0}{3}\right)^n . OCR^C (\frac{\sigma'_{vc}}{p_a})^n \qquad \text{Equation 5.2}$$

where p_a is the atmospheric pressure, $\alpha = 202$ is a parameter that depends on soil type, $K_0 = 0.69$ is the coefficient of lateral earth pressure at rest, n is equal to 1, OCR is the overconsolidation ratio, c is equal to 0.3 for clay with PI = 40 and σ'_{vc} is the vertical effective consolidation stress.

The undrained shear strength S_u was deduced from Ladd (1991) concept based on the following formulation:

$$\frac{S_u}{\sigma'_{vc}} = 0.22 * OCR^{0.8} \qquad \text{Equation 5.3}$$

The value of 0.22 represents the undrained strength ratio for a normally consolidated soil and it was deduced from a direct simple shear tests using the same reconstituted bay mud soil. The value of 0.8 was recommended from Ladd (1991). In order to study the effects of strain rate on the undrained shear strength of the bay mud, direct simple shear tests were performed at different strain rate. The results showed that the reconstituted bay mud has a shear strength that increases by 13 % with the logarithm of the strain rateranging from 0.01 %/s to 10 %/s (Figure 5.4). For more information on these tests, the reader is referred to Afacan et al. (2014.a,b)

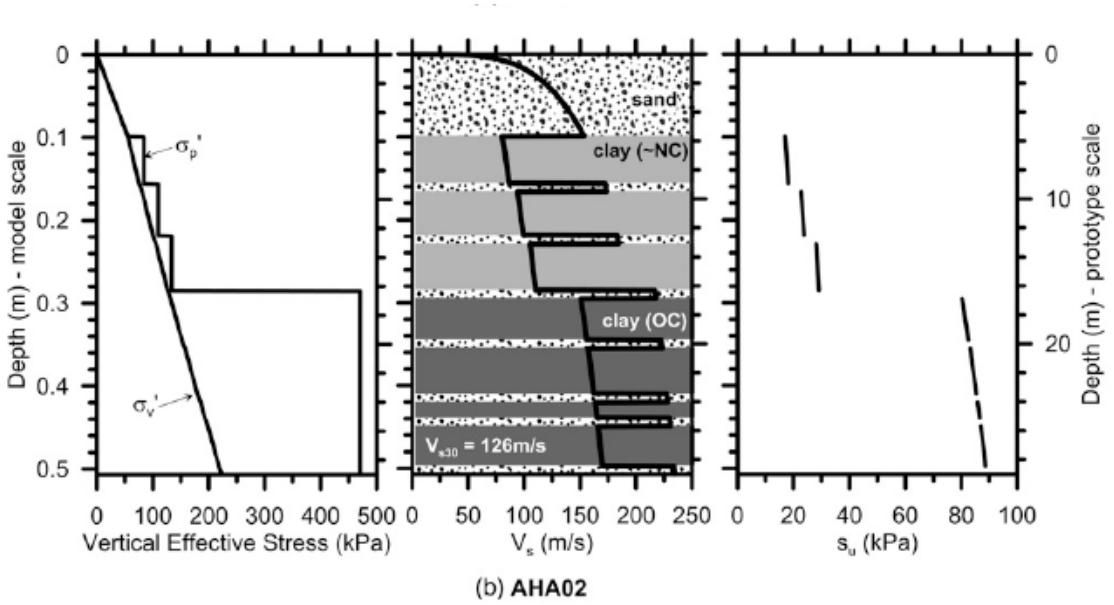

Figure 5.3 Properties of centrifuge model AHA02 (Afacan et al. 2014.a)

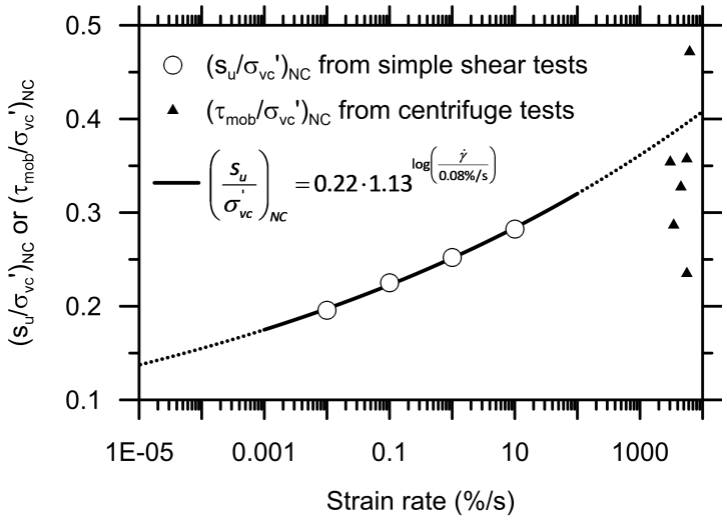

Figure 5.4 Increase of Shear strength with the logarithm of strain rate (Afacan et al. 2014b)

During the centrifugetests, strain-rates scale the g-levelconducted at 57g and can reach values up to 6,000 %/s in the model. This level of strain rate is about 60 times what is typically observed during earthquake loading in real-life. Regardless of the specificities of a centrifuge test regarding strain-rate, these levels of strain rate warrant a strain-rate correction of shear strength is necessary to avoid the underprediction of shear strength.

In order to provide a shear strength corrected modulus reduction curve, Afacan et al. (2014b) modified the modulus reduction curves obtained through the empirical relationships introduced

by Darendeli (2001) to match a target shear strength using the procedure from Yee et al. (2013). The curves were further modified to match a target rate-adjusted shear strength, and Afacan et al. (2014b) showed that the use of strain-rate-adjusted profiles of undrained shear strength allows to obtain more accurate predictions in ground response analysis. The centrifuge model was shaken with 19 earthquake ground motions with peak accelerations varying from 0.02g to 0.6g. Table 5.3 presents the characteristics of some of the seed ground motions used in the centrifuge tests. The motions used in the centrifuge tests were all scaled versions of these motions.

Table 5.3 Characteristics of ground motions used in centrifuge tests (Afacan et al. 2014a)

Earthquake	Record/component	M_w	R_{jb} (km)	V_{s30} (m/s)	PGA (g)	PGV (cm/s)	PGD (cm)
1979 Coyote Lake, CA	CYC160	5.7	5.3	597	0.157	10.8	1.3
1994 Northridge, CA	RRS228	6.7	0.0	282	0.838	166.1	28.8
1994 Northridge, CA	WPI046	6.7	2.1	286	0.455	92.8	56.6
1994 Northridge, CA	SCS142	6.7	5.4	251	0.897	102.8	47.0
1995 Kobe, Japan	NIS000	6.9	7.1	609	0.509	37.3	9.5
1995 Kobe, Japan	PRI090/KP4090	6.9	3.3	198	0.325	23.28	13.1
1989 Loma Prieta, CA	LGP090	6.9	0.0	478	0.605	51.0	11.5
1999 Hector Mine, CA	HEC000	7.1	10.4	685	0.266	28.5	22.5
1999 Chi Chi, Taiwan	TCU045-W	7.6	26.0	705	0.474	36.7	50.7

Note: Motion and record/component codes are from PEER-NGA database (Chiou et al. 2008).

5.3.3 Centrifuge model in Deepsoil

Afacan (2014) performed nonlinear ground response analysis on Deepsoil to study the performance of the existing modeling methods in predicting the site response observed in the centrifuge tests in prototype scale. In order to study the performance of the viscoplastic model, we compare its predictions with the ARCS model's in ground response analysis in Deepsoil. The same input parameters are used with both models and are as follows:

- Modulus reduction and damping curves corrected for monotonic shear strength, but not strain-rate corrected. This approach was chosen because the viscoplastic model includes in its formulation the strain-rate dependency. The curves were the same that Afacan (2014) used and the correction is described in the section above.
- Shear wave velocity, unit weight, taken from the information provided by Afacan (2014).
- D_{min} which represents the minimum damping ratio. This value is deduced from the damping curve.

- For the viscoplastic model, the desired increase in shear strength per logarithm of strain is needed as an additional parameter. This value was set as 13% for all clay layers in order to be consistent with the observations in the lab tests.

Profiles of input shear wave velocity, maximum propagable frequency and small strain damping are shown in Figure 5.5. Given that the motions recorded were directly used as input motions, a rigid bedrock was used to follow the recommendations from Hashash et al. (2016). To model small strain damping, the frequency independent damping formulation was used during analyzes. This formulation removes several of Rayleigh Damping limitations and does not require to select modes or frequencies (Phillips and Hashash 2009). Simulations were done and compared to the results of the centrifuge tests (Afacan et al. 2014b).

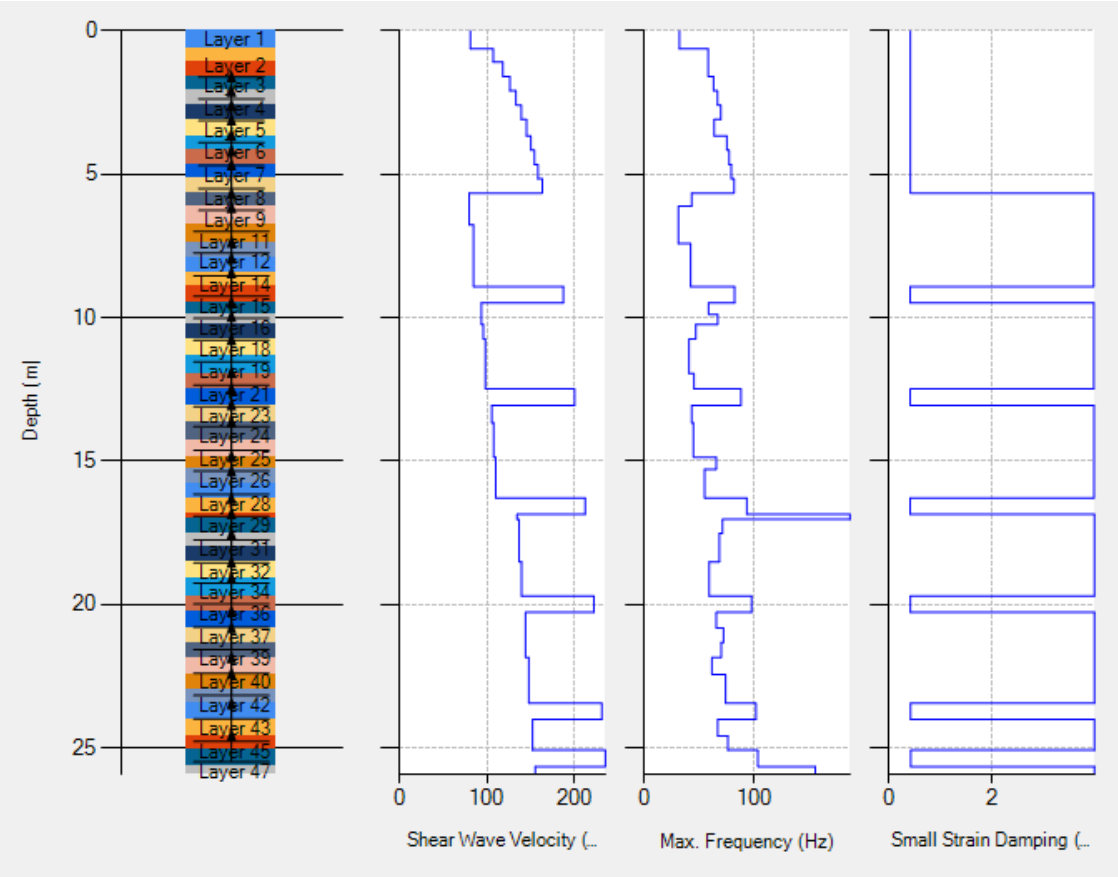

Figure 5.5 Properties of input soil (screenshot from Deepsoil)

5.3.4 Spectral comparison

The results of the simulations and the centrifuge tests are compared in terms of response spectra at a depth corresponding to the shallowest accelerometer in the centrifuge test. Figure 5.7 presents a comparison of the spectral accelerations of the surface layer, obtained with the two different models and measured in the centrifuge for a few input motions presented in Figure 5.6. The spectral response of the viscoplastic model is constantly closer to the spectral response of the centrifuge model compared to the ARCS model, both in terms of PGA and maximum spectral response. This trend was observed for all 19 motions that were tested, which illustrates that the strain rate dependency improves the predictions for nonlinear ground response analysis. It should also be noted that the period at which the maximum spectral acceleration was observed was not modified by the inclusion of the viscous effects even for motions where strong nonlinearities developed, such as motion 18.

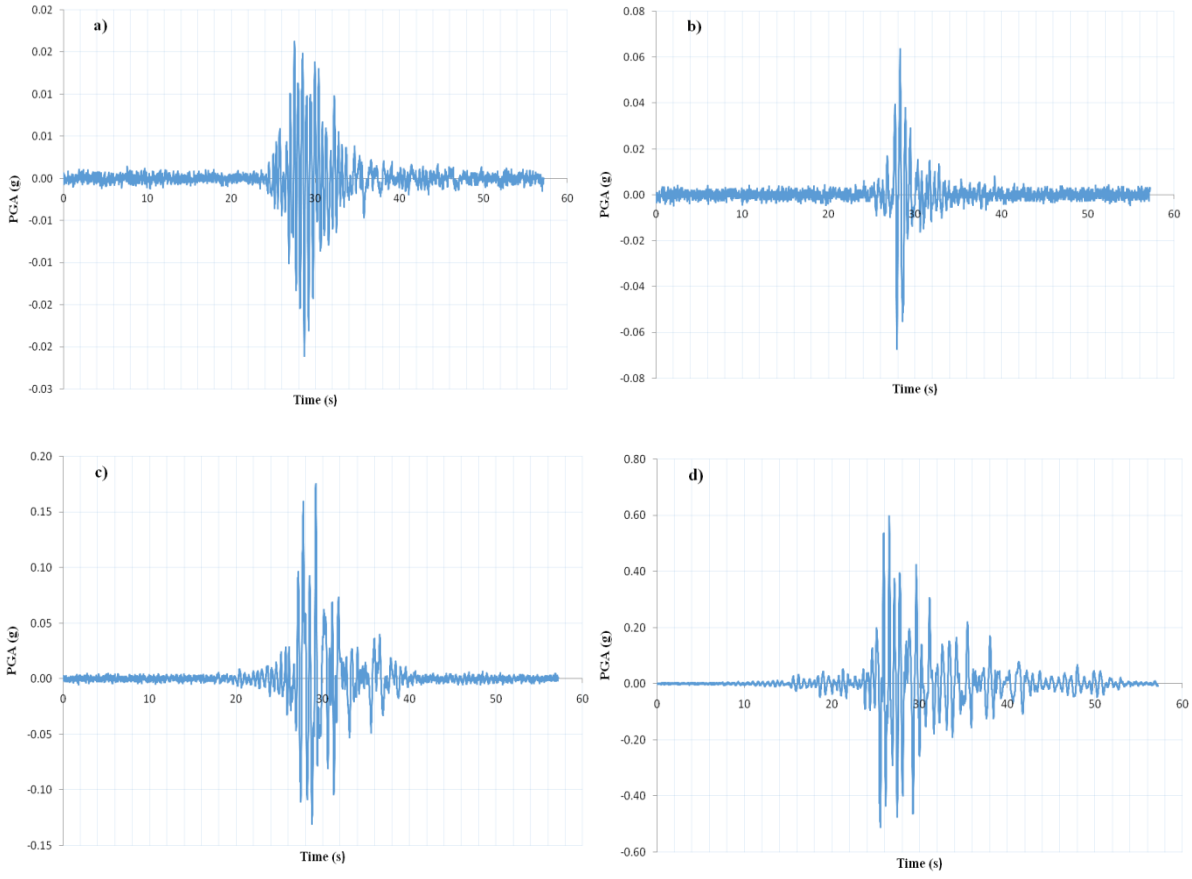

Figure 5.6 Acceleration time series used in the simulations a) Motion5 b) Motion7 c) Motion16 d) Motion18

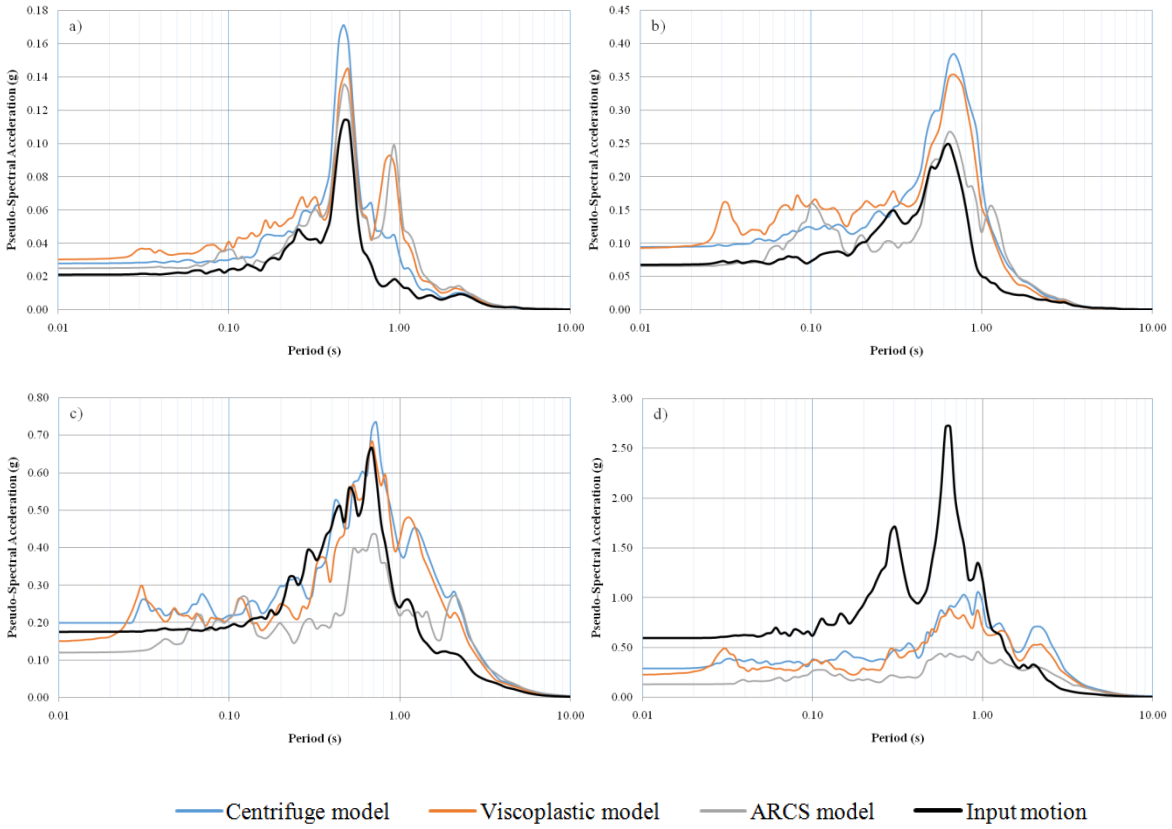

Figure 5.7Comparison of spectral accelerations on four different motions: a) Motion 5 b) Motion 7 c) Motion 16 d) Motion 18

5.3.5 Residual comparison

The results of all the simulations are better studied by comparing the residuals, defined as the difference between the observed and predictedintensity measures as defined in Equation 5.4:

$$R_i = \ln IM_{obs,i} - \ln IM_{sim,i} \qquad \text{Equation 5.4}$$

Where I is the number of the input motion and varies from 1 to 19, $IM_{obs,i}$ is the observed intensity measure for the input motion i and $IM_{sim,i}$ is the predicted intensity measure. The intensity measure studied here is the Pseudo Spectral Acceleration (*PSA)* calculated 100 periods between 0.01s and 10s. Figure 5.8 presents the residuals of *PSA* for the viscoplastic model and the ARCS model as a function of periods. Input motions with small amplitude (PGA_b < 0.1g) and medium to large amplitude (PGA_b > 0.1g) are separated, and median residuals are also plotted for both categories.

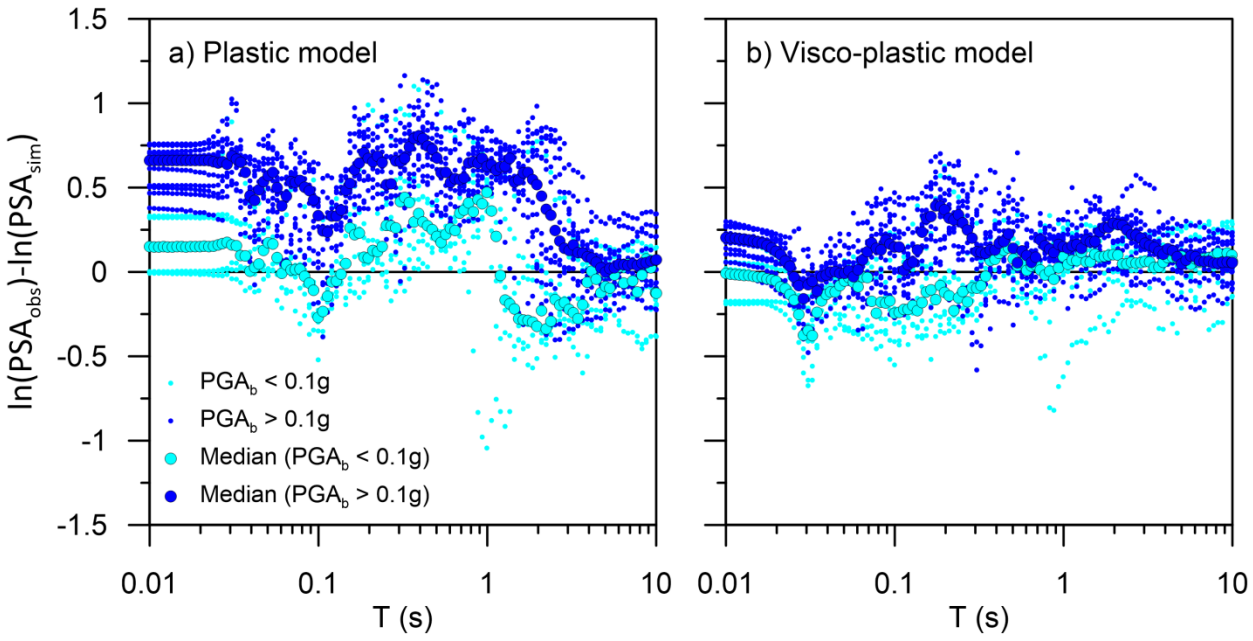

Figure 5.8PSA residuals for 19 input motions

The ARCS plastic model residuals are largely positive for input motions with $PGA_b > 0.1$g which indicates an overall under-prediction of ground motions caused by low shear strength and stiffness in the simulations because the lack of accountability of strain-rate effects. On average small-amplitude input motions ($PGA_b < 0.1$g) showed an under-prediction at short periods (positive residuals) and a slight but acceptable over-prediction (negative residuals) at periods longer than 1s. On the other hand, the viscoplastic model residuals showed better predictions for both large and small-amplitude motions at every period, even though the model shows a constant slight underprediction for large motions. For small-amplitude input motions ($PGA_b < 0.1$g) an over-prediction (negative residuals) at short period (0.01s to 0.3s) and under-prediction at periods longer than 0.3s is observed. However, for most periods and all motions, the viscoplastic model residuals are closer to zero comparing to the ARCS model residuals which means that the observed and predicted intensity measures are closer, showing that the strain rate effects added in the viscoplastic model improve the predictions of ground response analysis comparing to rate-independent ARCS model.

5.3.6 Transfer function comparison

Figure 5.9 presents a comparison of the transfer function of motions 7 and 13 with a peak acceleration of 0.06g and 0.24g respectively, obtained with the two different constitutive models

(viscoplastic and ARCS) and the centrifuge model. The transfer function is defined as the ratio of the fast fourier transform (FFT) of the output to the input acceleration. In the centrifuge test, the accelerometer is not able to measure precisely accelerations at frequencies lower than 0.3 Hz and the measurement at high frequencies is associated with significant noise because both the input and output motions have a low frequency content higher than 5 Hz. Both models are able to capture the peak of the transfer function for both motions even though they happen at different frequencies (1Hz for motion7 and 0.7 Hz for motion13). A comparison between the ARCS and the viscoplastic model shows that the two models are close, but that the latter seems to give slightly better predictions at frequencies between 0.2 and 2 Hz, which is the range of frequencies we are the most interested with, since the rest is heavily influenced by noise. It is noticeable that the peak amplitude at around 0.7 Hz observed in the centrifuge model is better captured for motion13, which seems to indicate that the added strain rate effects improve the predictions of ground response analysis, especially for larger motions.

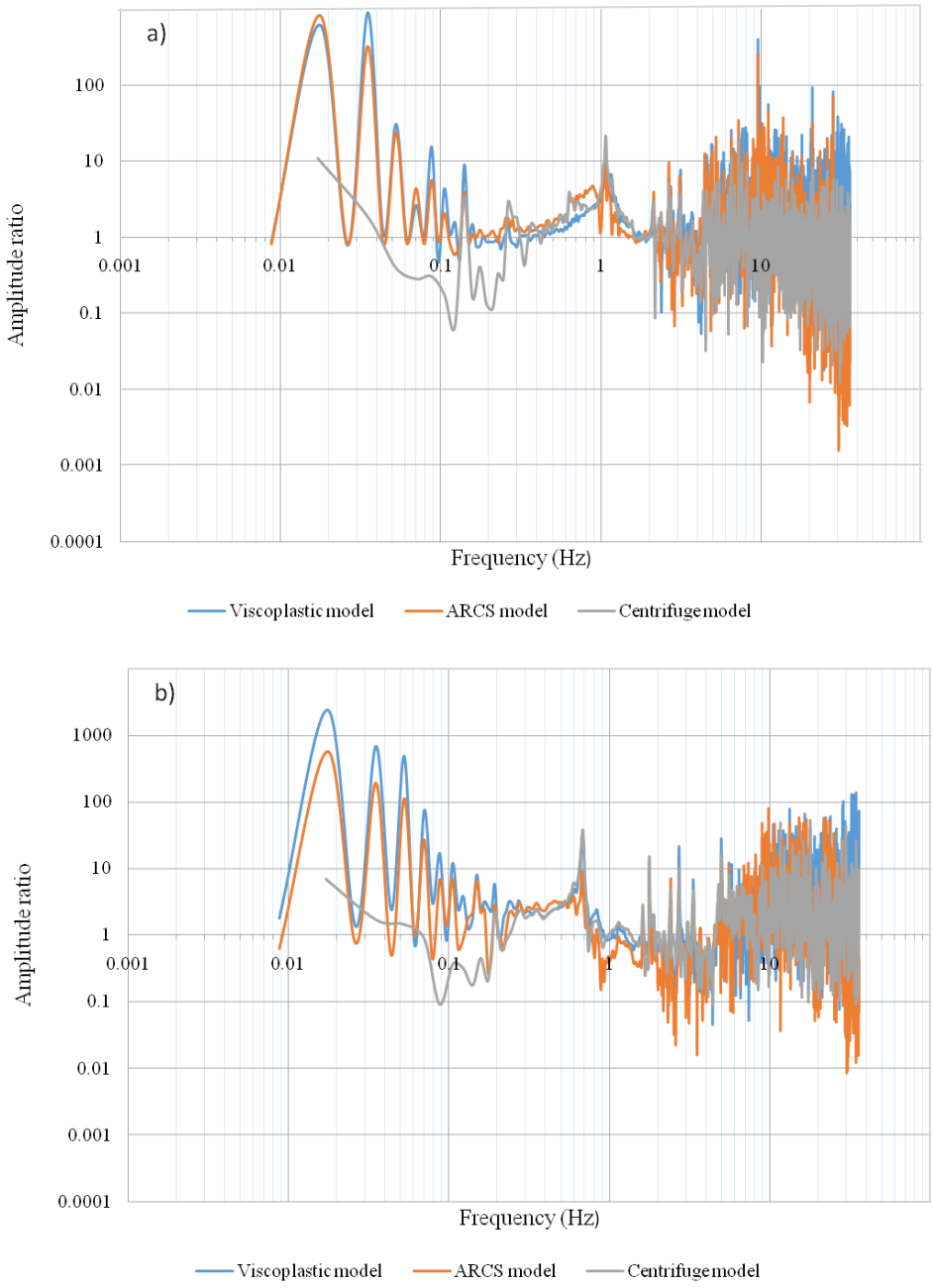

Figure 5.9 Comparison of transfer function a) Motion 7 b) Motion 13

CHAPTER 6 CONCLUSIONAND RECOMMENDATIONS

This chapter summarizes the findings of this research project with respect to the initial objective, which was to create a viscoplastic model for nonlinear 1D ground response analyses. The main contributions of this research project are stated and discussions on the limitations of the work and some suggestions for future work are presented.

6.1 Synthesis

A new viscoplastic model to be used in nonlinear 1D ground response analysis was presented. A review of literature of one-dimensional ground response analysis allowed to understand the theory of ground response analysis, the three methods used to model the soil behaviour (linear, equivalent linear and nonlinear), and a presentation of the main constitutive models used in nonlinear analysis. The different models were discussed through their ability to match or not the input modulus reduction and damping curves. Finally, an introduction of the viscous phenomena observed in the soil's behaviour was presented in order to understand the viscous effects on the mechanical response of soil, and several types of time-dependent models and their limitations were also presented.

Secondly, the constitutive equations of the viscoplastic model were presented. The total stress is divided into inviscid and viscous part. The inviscid part is based on the formulation of the Yniesta et al. (2017) 1D model that permits to match any target damping and modulus reduction curves. The viscous stress is formulated as a direct function of strain-rate $\dot{\gamma}$ which allows to capture the strain rate dependency of soils, based on a viscous coefficient c_{visc} that permits to control the desire increase of shear strength. A coefficient F is added to the formulation so that the model yields realistic stress-strain curves upon a variety of loading paths, when the viscous stress is added to the inviscid stress.

The constitutive equations were then validated using different examples of single element simulations. The model provides a good estimate of the viscous effects observed in laboratory tests during cyclic testing. In particular the model is able to capture well the strain-rate dependency of the shear strength with the logarithm of the strain rate which is consistent with Sheahan et al. (1996). The added viscous stress induces a higher hysteretic damping similarly to

Darendeli's (2001) observations. The effects of strain-rate, viscous coefficient c_{visc} and frequency on the stress-strain response and the hysteretic behaviour were also described.

Finally, the implementation of the viscoplastic model in the ground response analysis software Deepsoil was presented in order to validate the model in full ground response simulations. The results of 1D ground response analysis using the viscoplastic model were compared to centrifuge tests (Afacan et al. 2014), and the comparison with the predictions of the ARCS model confirmed that the viscoplastic model allows to have better predictions wave propagation in nonlinear ground response analysis whether the results are compared in terms of response spectra, residuals or transfer functions.

6.2 Contributions

The main contributions of this research project are the development of a constitutive model that integrates viscous effects in a realistic fashion, and its integration in a ground response analysis software. The model permits to integrate the effect of strain rate on the soil's behaviour in one dimensional site response analysis, which can significantly improve the predictions of ground motion propagation.

It was proved that the soil behaviour is strongly strain-rate dependent during both monotonic and cyclic loading, and unlike most nonlinear models, the viscoplastic model is able to capture these effects accurately. Simulations using the viscoplastic model have shown that the model is able to provide better predictions in nonlinear ground response analysis and can be used as an integrated model in the Deepsoil software to simulate ground response.

6.3 Limitations

The main limitation of the viscoplastic model is that the damping response is not fully controlled despite being realistic. The model provides an increase in hysteretic damping related to viscous effects that follow the trend observed by other researchers, but is not quantitively controlled.

The second limitation is that upon a sudden change of shear strain during earthquake loading, leading to large changes in strain-rates and large changes in viscous stresses, the model sometimes produces stress-strain curve that presents a slightly convex shape, which is unrealistic.

However, this was not observed in most simulations performed, and the effect on the final results is essentially negligible.

6.4 Future work

The presented model could be modified so that a sudden change of shear strain during earthquakes would yield a more realistic shape of the stress-strain curve. To do so, a comparison between the current and the previous shear strain should be done and as soon as an important gap is noticed, the viscous stress should be attenuated in order to obtain a realistic stress-strain curve.

Once the model will be improved, it could be further extended to 3D conditions. Developing a 3D constitutive model based on the 1D viscoplastic model will allow to include viscous effects in multidimensional site response analysis.

REFERENCES

Afacan, K. (2014). “Evaluation of nonlinear site response of soft clay using centrifuge models.” Ph.D. thesis, University of California, Los Angeles, CA.

Afacan, K., Brandenberg, S., and Stewart, J. (2014a).“Centrifuge modeling studies of site response in soft clay over wide strain range.”*Journal of Geotechnical and Geoenvironmental Engineering* (ASCE) GT.1943-5606.0001014

Afacan, K.,Yniesta, S.,Shafiee, A., Stewart, J., Brandenberg, S. (2014b). “Total stress analysis of soft clay ground response in centrifuge models.” *Journal of Geotechnical and Geoenvironmental Engineering* (ASCE)

Augustesen, A., Liingaard, M. and Lade, P. V. (2004). “Evaluation of time dependent behavior of soils.” *International Journal of Geomechanics*4 (3): 137–156.

Borja, R.I., Lin,C.H.,Sama, K.M., Masada, G.M. (2000) “Modelling non-linear ground response of non-liquefiable soils” Earthquake Engineering and Structural Dynamics, 29 (1), pp. 63-83

Darendeli, M. (2001). “Development of a new family of normalized modulus reduction and material damping curves.” Ph.D. Thesis, Dept. of Civil Eng., Univ. of Texas, Austin.

Duvant, G. & Lions, I.J. (1972) “ Les inequations en mecanique et en physique. ”Paris, France :Dunod.

Kulhawy,F. H. and Mayne, P. W. (1990)“Manual on estimating soil properties for foundation design.”Report L-6800, Electric Power Research lnstitute , Palo Alto. Calif.

Graham, J., Crooks, J. H. A. and Bell, A. L. (1983). “Time effects on the stress-strain behavior of soft natural clays.”Geotechnique, 33(3), 327-340.

Groholski, D.R.,Hashash, Y.M., Kim, B., Musgrove, M., Harmon, J., and Stewart J.P. (2016). “Simplified model for small-strain nonlinearity and strength in 1D seismic site response analysis”*Journal of Geotechnical and Geoenvironmental Engineering*. 142, 4016042.

Hardin, B.O. and Drnevich, V.P. (1972). “Shear modulus and damping in soils: designequations and curves,” Journal of the Soil Mechanics and Foundations Div., ASCE, 98(SM7), 667–692

Hashash, Y.M.A. and Park, D. (2001). "Non-linear one-dimensional seismic ground motion propagation in the Mississippi embayment," *Engineering Geology*, 62 185–206

Hashash, Y. M. A., Phillips, C., and Groholski, D. R. (2010) "Recent advances in non-linearsite response analysis." *Fifth International Conference on Recent Advances inGeotechnical Earthquake Engineering and Soil Dynamics, San Diego 2010.*

Hashash, Y. M. A., Musgrove, M. I., Harmon, J. A., Groholski, D.R., Phillips, C., and Park, D., (2016). DEEPSOIL 6.1, User Manual.

Isenhower, W.M. and Stokoe, K.H. (1981) "Strain-rate dependent shear modulus of San Francisco bay" InternationalConferences on Recent Advances in Geotechnical Earthquake Engineering and Soil Dynamics, Volume II, 597-602, St. Louis

Kaklamanos, J., Bradley, B.A., Thompson, E.M. &Baise, L.G. (2013). "Criticalparameters affecting bias and variability in site-response analyses using KiKnetdownhole array data."*Bulletin of the Seismological Society of America*, 103(3), 1733-1749

Kaklamanos, J., Baise, L.G., Thompson, E.M., &Dorfmann, L. (2015). "Comparison of1D linear, equivalent-linear, and nonlinear site response models at six KiK-netvalidation sites" *Soil Dynamics and Earthquake Engineering 69, 207-219.*

Konder, R.L and Zelasko, J.S. (1963), "Hyperbolic stress-strain formulation of sands", Second Pan American conference on soil mechanics and foundation engineering, Saopaulo, Brazil, pp289-324.

Kutter,B. L. and SathialingamN., (1992) "Elastic - viscoplastic modelling ofthe rate-dependent behaviour of clays". *Geotechnique*. Vol. 42, no. 3, p.427-441.

Kutter,B.L. (1992)"Dynamic centrifuge modeling of geotechnical structures". Transportation Research Record, TRB, National Research Council, 1336: 24-30.

Ladd, C.C. (1991). "Stability evaluation during staged construction," *Journal of Geotechnical Engineering.*, 117(4), 540–615.

Lefebvre, G. and LeBoeuf, D. (1987). "Rate effects and cyclic loading of sensitive clays,"*Journal of Geotechnical Engineering*, 113(5), 476-489.

Liingaard, M., Augustesen, A. and Lade, P.V., (2004). “Characterizationof models for time-dependent behavior of soils.”*InternationalJournal of Geomechanics*, 4 (3), 157–177.

Liu, M., and Gorman, D.G. (1995). "Formulation of Rayleigh damping and its extensions."*Computers and Structures*, 57(2), 277-285.

Mac, N., Shahbodaghkhan, B., Khalili, N.(2014), “A Constitutive model for time-dependent behavior of clay”, *International Journal of Civil, Structural, Construction and Architectural Engineering Vol:8, No:6, 2014*

Masing, G. (1926). “Eigenspannungen and verfertigungbeim messing.” *Proc. 2nd Int. Congress on Applied Mech.*, Zurich, Switzerland

Matasovic, N. and Vucetic,M. (1993). “Cyclic characterization of liquefiable sands,” *Journal of Geotechnical Engineering.*, ASCE, vol 119 No 11, 1805-1822

Menq, F.Y. (2003) “Dynamic properties of sandy and gravelly soils”, Ph.D. thesis, University of Texas at Austin, TX, USA, 364.

Newmark, N.M. (1959). “A method of computation for structural dynamics,” *Journal of the Engineering Mechanics Division.*, ASCE, 67-94

Olszak, W., and Perzyna, P. (1966). ‘‘The constitutive equations of theflow theory for a nonstationary yield condition.’’ *Proc., 11th Int. Congressof Applied Mechanics*, Springer, Berlin, 545–553.

Pruiksma, J.P. (2016). “Nonlinear and equivalent linear site response analysis for the Groningen area”. TNO report, R10460, Delft, the Netherlands.

Park, D. and Hashash, Y.M.A. (2004). “Soil damping formulation in nonlinear time domainsite response analysis,” *Journal of Earthquake Engineering*, 8(2), 249-274.

Phillips C. and Hashash Y. M. A. (2009) “Damping formulation for nonlinear 1D siteresponse analyses.” *Soil Dynamics and Earthquake Engineering*, 29(7), 1143-1158.

Pyke, R.M. (1979). “Nonlinear soil models for irregular cyclic loadings,” *Journal of Geotechnical Engineerin.*, ASCE, 105(GT6), 715-726.

Pyke, R.M. (2000). *TESS: A computer program for nonlinear ground response analyses*. TAGA Engineering Systems & Software, Lafayette, Calif.

Rayleigh, J.W.S and Lindsay R.B. (1945). *The theory of sound, Dover Publications*, NewYork

Richardson, A.M. & Whitman, R.V. (1963). “Effect of strain-rate upon undrained shear resistance of a saturated remoulded fat clay”. Geotechnique 13, No. 4, 310–324

Ridders C.J.F. (1979) “A new algorithm for computing a single root of a real continuous function.” IEEE Transactions on circuits and systems, 979-980.

Seed, H.B., and Idriss, I.M. (1969). "Influence of soil conditions on ground motions duringearthquakes." *ASCE Journal of the Soil Mechanics and Foundations Division*, 95, 99-137.

Sheahan, T.C., Ladd, C. C., & Germaine, J. T. (1996). “Rate-dependent undrained shear behavior of saturated clay.” *Journal of Geotechnical Engineering*, *122*(2), 99-108.

Stewart, J.P., Kwok, A.O., Hashash, Y.M.A., Matasovic, N., Pyke, R., Wang, Z., and Yang, Z.(2008). "Benchmarking of nonlinear geotechnical ground response analysisprocedures," *Report PEER 2008/04*, pacific Earthquake Engineering Research Center,University of California, Berkeley.

Vucetic, M., Lanzo, G. and M. Doroudian (1998). “Damping at small strains in cyclic simple shear test.” *Journal of Geotechnical and Geoenvironmental Engineering*, ASCE, 124(7), 585-594.

Yee E., Stewart J.P., Tokimatsu K. (2013) “Elastic and large-strain nonlinear seismic siteresponse from analysis of vertical array recordings”, *Journal of Geotechnical and Geoenvironmental Engineering*, 139 (10), 1789-1801.

Yin, J.H., and Graham, J. (1994). ‘‘Equivalent times and onedimensionalelastic visco-plastic modelling of time-dependent stress strainbehaviour of clays.’’ *Canadian GeotechnicalJournal*, 31, 45–52.

Yin, J.H., and Graham, J. (1996). ‘‘Elastic visco-plastic modelling of one-dimensional consolidation.’’ *Geotechnique*, 46(3), 515–527.

Yin, J. H. (1999). ‘‘Nonlinear creep of soils in oedometer tests.’’ *Geotechnique*, 49(2), 699–707.

Yniesta,S., Brandenberg, S. J., and Shafiee, A. (2017). "ARCS: A one dimensional nonlinear soil model for ground response analysis."*Soil Dynamics and Earthquake Engineering*, 102, 75-85.